Master Thesis

Activation and co-substrate utilization of lytic polysaccharide monooxygenases

UNIVERSITY OF NATURAL RESSOURCES AND LIFE SCIENCES, VIENNA
Department of Food Sciences and Technologies
Institute of Food Technology

NORWEGIAN UNSIVERSITY OF LIFE SCIENCES, ÅS
Fakultet for kjemi, bioteknologi og matvitenskap
Protein Engineering and Proteomics group

This project was done under supervision of:
Supervisor: Priv.-Doz. Dipl.-Ing. Dr. Roland Ludwig
Co-supervisor: Dipl.-Ing. Dr. Daniel Kracher

Sonja Gangl, BSc — 01.12.2017

VerfasserIn — Datum

Master Thesis

Activation and co-substrate utilization of lytic polysaccharide monooxygenases

Eingereicht von: Sonja Gangl, BSc

Matrikelnummer: 1240087

am: 01.12.2017

Master study in Biotechnology

Universität für Bodenkultur Wien

Eidesstattliche Erklärung der Verfasserin

Ich erkläre ehrenwörtlich, dass ich die Arbeit selbständig angefertigt, keine anderen als die angegebenen Hilfsmittel benutzt und alle aus ungedruckten Quellen, gedruckter Literatur oder aus dem Internet im Wortlaut oder im wesentlichen Inhalt übernommenen Formulierungen und Konzepte gemäß den Richtlinien wissenschaftlicher Arbeiten zitiert, durch Fußnoten gekennzeichnet bzw. mit genauer Quellenangabe kenntlich gemacht habe. Diese Arbeit wurde in gleicher oder ähnlicher Form noch bei keinem/r anderen Prüfer/in als Prüfungsleistung eingereicht. Mir ist bekannt, dass die Verwendung unerlaubter Hilfsmittel rechtliche Schritte nach sich ziehen kann.

_____ _____

Datum Unterschrift

Acknowledgements

My sincere thanks go to my supervisor Roland Ludwig and my co-supervisor Kracher for their support throughout the whole master thesis.

Thanks to the great collaboration with the Norwegian University of Life Sciences, I had the exceedingly good opportunity to do parts of the thesis in the excellent group of Vincent Eijsink. I would like to express my sincere gratitude to Zarah Forsberg who helped me a lot and acted as another great co-supervisor during my stay in Ås.

Kurzzusammenfassung:

Da der Gedanke der Nachhaltigkeit und des Umweltschutzes einerseits in der Politik, in Form internationaler Klimaziele zur Bekämpfung bzw. der Zurückdrängung der Erderwärmung, andererseits aber auch in der Wirtschaft immer höhere Priorität erlangt, gilt es alternative, nachwachsende Rohstoffe zu erforschen. Ein zukunftsweisender Weg ist der Abbau von Zellulose oder Chitin, welches in großen Mengen in der Natur verfügbar ist, mit einem Enzym lytische Polysaccharidmonooxygenase (LPMO). Dieses Enzym verstärkt die Wirkung von Hydrolasen, welche die Bausteine dieser Polymere freisetzen. Diese Mono-, di- und Oligosaccharide können zur Erzeugung von Biotreibstoffen und neuen natürlichen Polymeren verwendet werden.

Leider sind von der LPMO nur sehr wenig kinetische Daten verfügbar. Im Zuge dieser Arbeit wurde eine elektrochemische Methode basierend auf der Detektion des Wasserstoffperoxids, einem möglichen Substrat der LPMO, entwickelt. Diese Methode misst online und in Echtzeit. Die katalytischen Raten der Substratumsetzung konnten damit bestimmt werden. Diese Arbeit zeigt, dass sich die Umsatzgeschwindigkeit von LPMO verlangsamt, wenn das stöchiometrische Verhältnis zum Hilfsenzym Cellobiosedehydrogenase (CDH) abnimmt.

Mit dem Fokus auf die Aktivierung der LPMO Aktivität, wurden vier verschiedene *Myriococcum thermophilum* CDH Varianten, *Mt*CDH IIA, *Mt*DH IIA, *Mt*CDH Oxy^+ und *Mt*DH Oxy, getestet. Bei den Varianten *Mt*DH IIA und *Mt*DH Oxy^+ handelt es sich um Einzeldomänen der CDH, die nur den katalytisch aktiven Dehydrogenase (DH) Teil umfassen. Die Aktivierung mit *Mt*CDH Oxy^+ funktionierte dabei so gut, dass die Menge an CDH um einen Faktor von 47 im Verhältnis zur notwendigen Menge an *Mt*CDH IIA reduziert werden konnte um die gleiche Menge an Zellulose- und Chitinoxidationsprodukten herzustellen.

Entgegen dem aktuellen Stand der Forschung wurde mit der Verwendung von HPAEC zur Quantifizierung von LPMO Produkten gezeigt, dass Zelluloseoxidationsprodukte von der DH Domäne produziert werden. Hypothesen zur Erklärung dieser Beobachtung wurden in dieser Arbeit getestet.

Schlagwörter: LPMO, CDH, LPMO-Aktivierung, Enzymkinetik, Elektrochemie, Oxidative Depolymerisierung

Abstract:

As society, politics and industry is more and more concerned about sustainability and environmental protection, the efforts are increased to reach international climate goals and to control global warming. This is done by saving resources and finding alternative, renewable resources, especially non-edible plant carbohydrates. A promising way to degrade cellulose or chitin, which is available in great amounts in nature is lytic polysaccharide monooxygenase (LPMO). This enzyme supports other recalcitrant material degrading hydrolases to release easily accessible building blocks to generate biofuels or new polymers. LPMOs can not only support other hydrolytic enzymes, but also release mono-, di- and oligosaccharides themselves.

Unfortunately, only limited kinetic data on LPMOs are available. During this thesis, an electrochemical method was established, based on H_2O_2, which is consumed by LPMO. This method is performed online and in real time. Catalytic rates for the substrate consumption were determined. The enzyme was either activated ascorbic acid or cellobiose dehydrogenase (CDH) by providing electrons. This thesis shows that the reaction rate of LPMO decreases with decreasing availability of CDH.

To focus on the activation of the peroxygenase activity of LPMO, four different Myriococcum thermophilum CDH variants, variants *Mt*CDH II, *Mt*DH IIA, *Mt*CDH Oxy^+ and *Mt*DH Oxy^+, were tested. *Mt*DH IIA and $^+$ *Mt*DH Oxy^+ are single domains of CDH, containing only the catalytically active dehydrogenase (DH) domain. The activation with *Mt*CDH Oxy^+ worked so well, that the concentration of enzyme could be reduced by a factor of 47 compared with *Mt*CDH IIA and still lead to same amounts of formed cellulo- or chito-oligosaccharides.

Contrary to the state-of-the-art it was shown by using HPAEC to quantify LPMO products, that LPMO products were formed by using only the DH domains. Hypotheses to explain this fact were tested, but no satisfying explanation was found. More research needs to be done to solve this observation.

Keywords: LPMO, CDH, LPMO-activation, enzyme kinetics, electrochemistry, oxidative depolymerisation

TABLE OF CONTENTS

1 Inhalt

1 Introduction

1.1 Second generation biofuels

The availability of fossil fuels will be limited in the foreseeable future, which will cause major structural changes in the global economy. (1) To establish a secure economy built on sustainability and low-carbon emissions it is inevitable to use second generation biofuels derived from non-edible biomass. (2)

First generation biofuels derived from starch or sugar cause a reliance on food as an energy source, which leads to a food vs. fuel conflict. As food is limited, it is an ethical predicament to satisfy future energy needs based on farmland dedicated for food, and alternatives are required.(2) Non-edible, woody plants are an alternative resource to derive so called second generation biofuels. (2) Plant biomass is the largest source of carbon on earth. (3) Lignocellulose, which is a major component in the secondary cell walls of plants, makes up the bulk of its mass Lignocellulose is a recalcitrant material composed of a complex mixture of cellulose, hemicelluloses and lignin (4) and forms the woody part of plants. Cellulose is formed from long chains of β-1,4-linked glucose units. The fully equatorial confirmation of ß-linked glucopyranose residues stabilizes the chair structure. Flexibility is minimized. Cellulose is a straight chain polymer and hydroxyl groups on glucose chains from a hydrogen bond with oxygen atoms from another chain. Degree of polymerization of cellulose as a synonym to its chain length and influences many properties. (5) Hemicelluloses are heteropolymers that include xylan, arabinoxylan, glucuronoxylan, xyloglucan and glucomannan. (6) Lignin is an aromatic polymer formed from *p*-coumaryl, coniferyl and sinapyl alcohols. (4) Lignocellulose is the most abundant biopolymer on earth. (7) As lignocellulose is an inert material, its controlled deconstruction for conversion into fuel is a technological challenge.(2) So called bio-refineries seek to degrade biomass down into its molecular components, which can be converted to biogenic fuels, or other chemicals and hydrocarbons. (8)

The most economically friendly way to degrade wood is the biochemical degradation relying on enzymes. (2) In nature, plant biomass is degraded by

microbial plant degraders, such as wood-rotting fungi. Decomposer fungi degrade the most recalcitrant organic polymers in plant cell walls into simple sugars. Fungi use specific sets of enzymes including carbohydrate-active enzymes with specialized catalytic activities. (4) Amorphous cellulose is degraded by endo-glucanases which induce chain breaks. These are access points for exo-enzymes like cellobiohydrolases. These enzymes release cellobiose, which is finally converted to glucose by glucosidases.(4) The recently discovered lytic polysaccharide monooxygenases are a particularly important class of enzymes in this process, as they catalyze the oxidative cleavage of glyosidic bonds in crystalline cellulose. It represents a promising enzyme for industrial biomass production, as it enhances the activity of cellulases. (9)

1.2 Lytic polysaccharide monooxygenases

LPMOs are copper-dependent enzymes cleaving glyosidic bonds in polysaccharides after activation by an electron donor. (10) These enzymes can hydroxylate the C1 and/or the C4 positions of scissile glyosidic bonds, which breaks the C-H linkage. (11) LPMOs are already used in industry, e.g. for the production of cellulosic ethanol, and are be of major importance for the industrial and biological biomass degradation. (12)

1.2.1 Classification

LPMOs are active on chitin, cellulose, hemicellulose, starch and soluble cello-oligosaccharides. (13) Based on sequence similarity LPMOS are classified in the Carbohydrate Active Enzyme (CAZy) database (www.cazy.org) into Auxiliary Activity families 9, 10, 11 and 13. (14) This database is a collection of enzymes and their associated carbohydrate binding modules.(15) LPMOs were originally classified as glycoside hydrolase family 61 (GH61), which consists of fungal enzymes. Originally, these enzymes were thought to have weak endoglucanase activity. Additionally, family 33 carbohydrate binding modules with similar structural features were identified in bacteria. (16) These AA10-type LPMOs can be found in eukaryotes, prokaryotes and viruses, in contrast to AA9, AA11 and AA13-type LPMOs which are exclusively found in fungi. (17)

1.2.2 Structures

A common structural feature of LPMOs is a fibronectin-like/immunoglobulin-like β-sandwich core structure consisting of 2 β-sheets comprising several β-strands and a catalytic histidine brace involved in copper coordination. (9) The structure is visible in Figure 1.

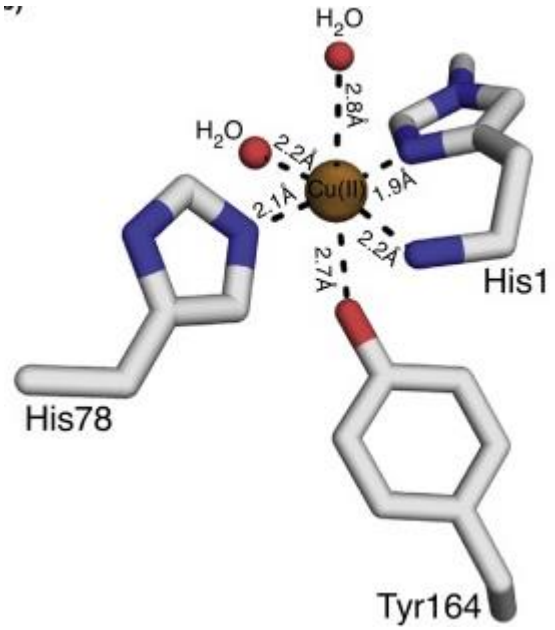

Figure 1. The active site of LPMO9 in its oxidized state, showing octahedral geometry. Amino acid side chains are shown as grey sticks.

The helices and loops that connect the core β-strands cause structural diversities between LPMOs of different families. This affects substrate interaction surfaces. The catalytic centre of chitin-active LPMOs contains a strictly conserved glutamate approximately 5 Å away from the active site copper. This residue is essential for catalysis and may be involved in the LPMO reaction mechanism. (18) The catalytic copper centre is strictly conserved in all LPMOs, as seen in Figure 2. whereas the rest of the substrate binding region is more diverse. Fungal LPMOs typically display aromatic several amino acids on the substrate-binding surface. The spacing between these corresponds to the distance separating monosaccharides in a polysaccharide chain, suggesting that they interact with the substrate. (9)

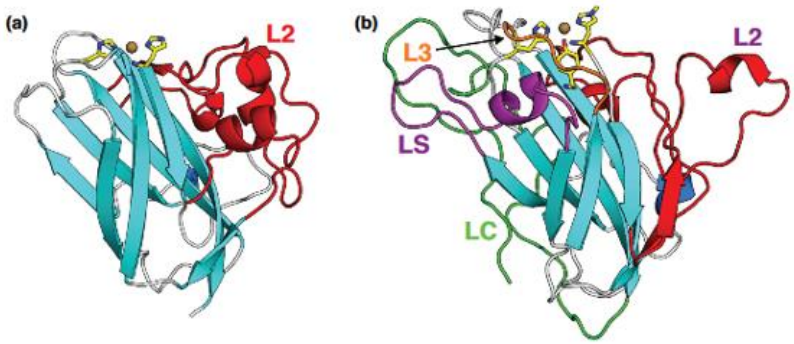

Figure 2. Structural diversity of LPMOs a) CBP21 b) *Nc*LPMO9c. L2, LS, and LC are important loops forming the substrate-binding surface. (9)

1.2.3 Reaction mechanism

The detailed reaction mechanism of LPMO is not known. However, several reaction pathways have been proposed. It is generally accepted that the resting redox state of the LPMO copper centre is Cu(II), which is reduced to Cu(I) after reductive activation. A longstanding hypothesis proposed that the reduced enzyme binds and activates dioxygen resulting in an oxyl, superoxo or peroxo intermediate. Hydrogen is abstracted from one of the carbons in the scissile glycoside bond, which could either be C1 or C4 in the case of cellulose. Hydroxylation of the resulting substrate radical leads to a destabilization and cleavage of the glyosidic linkage. (19) This reaction requires two electrons delivered by an external electron donor. There are many possible electron suppliers, either enzymes like fungal cellobiose dehydrogenases, or non-enzymatic activators derived from lignin breakdown products. (20)

According to a recently published paper (21) an H_2O_2-derived oxygen atom, rather than atmospheric oxygen is introduced into the polysaccharide chain. Following this hypothesis, a "priming" reduction of the LPMO Cu(II) to LPMO Cu(I) occurs first. H_2O_2 binds to Cu(I) and produces a Cu(II) hydroxyl or oxyl radical species after elimination of a water molecule. The Cu(II)- hydroxide-species attacks the C-H bond in cellulose leading to hydroxylation of the substrate and regeneration of the catalytic centre of LPMO to Cu(I). Bond cleavage occurs after molecular rearrangement to form a lactone (C1 oxidizer) or a ketoaldose (C4 oxidizer). Using controlled H_2O_2 supply stable reaction kinetics and higher enzymatic rates than with oxygen were reported. Bissaro et al. (21)

concluded that H_2O_2 and not oxygen is to be the catalytically relevant co-substrate of LPMOs.

1.2.4 Product formation

LPMOs are active on various plant polysaccharides including cellulose, soluble oligosaccharides, xyloglucans, starch and chitin. (13) A reaction mechanism as described above leads to hydroxylation of either the C1 or C4 glyosidic carbon, resulting in bond cleavage and a non-oxygenated product. Chitin-active LPMOs are strict C1 oxidizers while fungal LPMOs show activity on both the C1 and C4 position. A notable example of a C4-oxidizing enzyme is *Nc*LPMO9C from *Neurospora crassa*, which is also active on soluble oligosaccharides and several hemicelluloses. The reaction products are oxidized cellulose, as well as soluble oligosaccharides containing reducing and non-reducing ends.(Figure 3. and Figure 4.) (13)

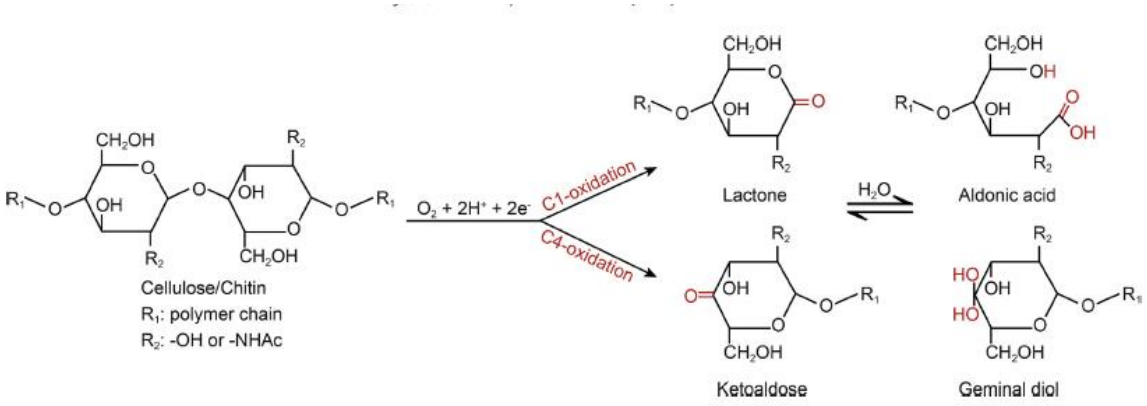

Figure 3. Reaction mechanism of LPMO on chitin and cellulose (22). Aldonic acid = Glc_nGlc1A; Ketoaldose = $Glc4KClc_n$; Gemdiol = $Glc4GemGlc_n$. When this figure was created, oxygen was thought to be the substrate of LPMO. According to state of the art research (21) this should be changed to H_2O_2.

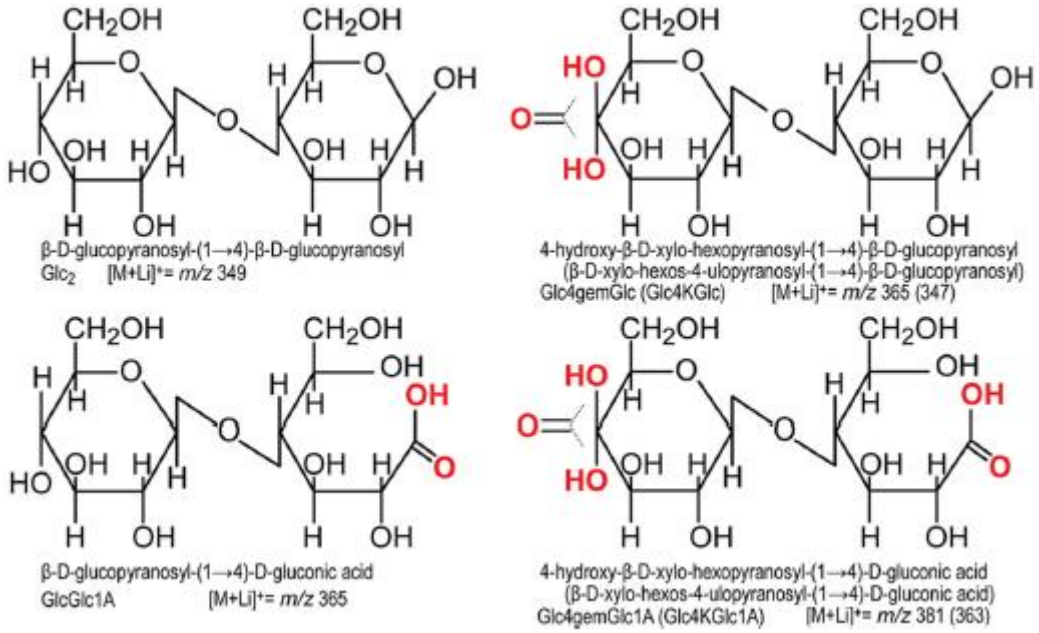

Figure 4. Overview of cellobiose oxidations. Oxidations are shown in red. IUPAC names, abbreviations and m/z values for the lithium adducts detected in these experiments are provided below the structures.(13)

Typical reaction products of *Nc*LPMO9C are soluble oligosaccharides which are dimers, trimers, and tetramers. These sugars are difficult to identify and quantify using standard methods, such as HPLC, due to their low abundance and oxidation at C4. One hexamer cluster of CBP21 is seen in Figure 5.

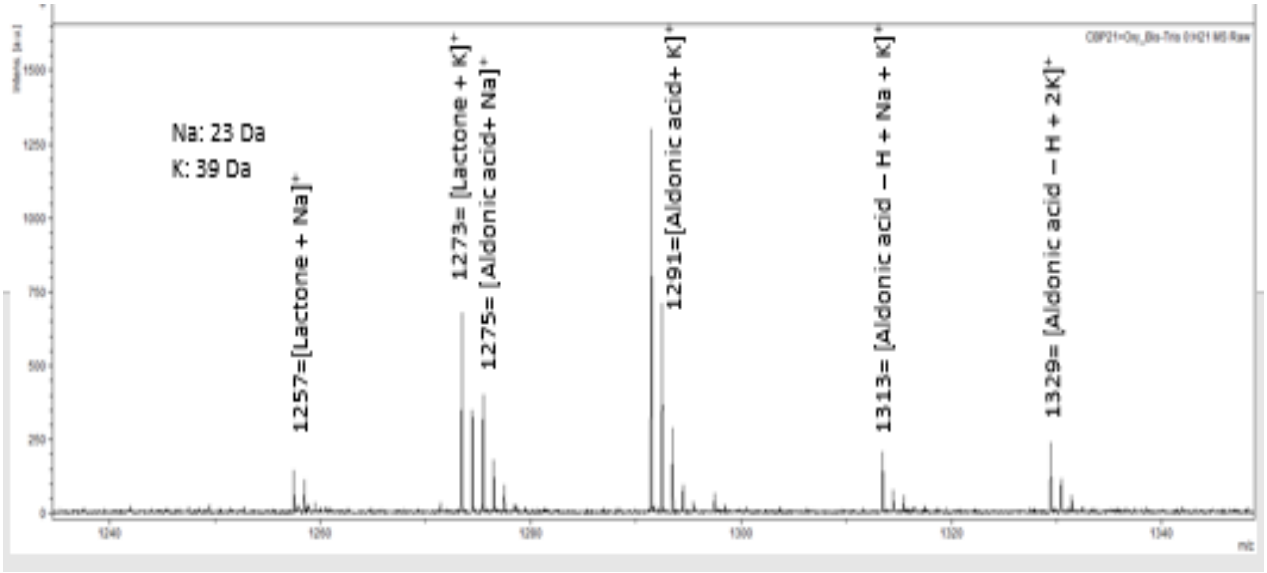

Figure 5. hexamer cluster CBP21. MALDI-TOF spectrum. As Bis-Tris buffer was used sodium and potassium adducts got visible. This sample is higher saturated with potassium as those peaks are higher.

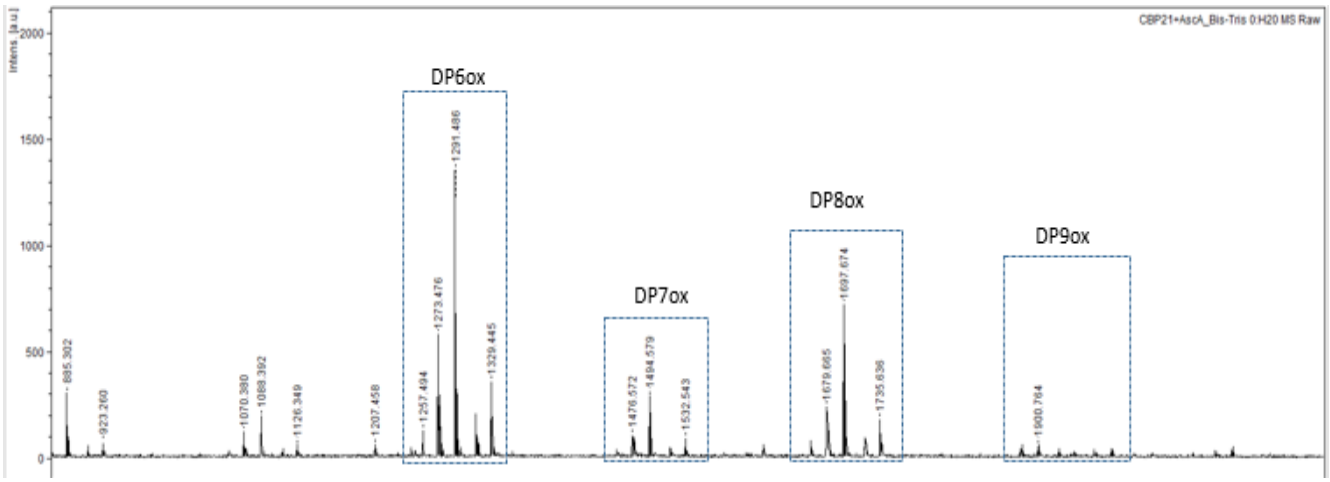

Figure 6. CBP21 in Bis-Tris buffer showing polymerization cluster from DP 6 to 9.

Analysis of LPMO products is very difficult, even at a qualitative level, due to the complexity of the products. Autoxidation of reactants may occur due to the pH instability of C4/C1 oxidized products generated from the reaction of C4 oxidizing LPMOs in combination with CDH, which oxidizes cellobiose and higher cello-oligosaccharides at C1. Moreover, the chromatographic analysis takes 50 min per sample to analyse products of *Nc*LPMO9C compared to an analysation time of 6 min per run for chitin active LPMOs products.

Other than for C4 oxidizers, there is a rapid and reproducible method available to quantify products of chitin-active C1 oxidizers. This method is based on copper saturation of LPMO combined with a fast-chromatographic method.

1.2.4.1 Quantitative product analysation of LPMO products

To obtain a simple product profile for chitin active LPMOs, the product mixture can be treated with chitobiase. Chitobiase is a member of N-acetylhexoaminidase family 20 and is able to hydrolyze soluble products. (22) Chitobiase operates by an exo-mechanism. It releases sugar moieties from the non-reducing end of the sugar chain and hydrolyzes chito-oligosaccharides. The digested product mixture only comprises GlcNAc and chitobionic acid, which is quantifiable using different HPLC methods as seen in Figure 7. As the open ring structure of chitobionic acid prevents it from enzymatic degradation, it is the only chito-oligosaccharide escaping chitobiase activity.

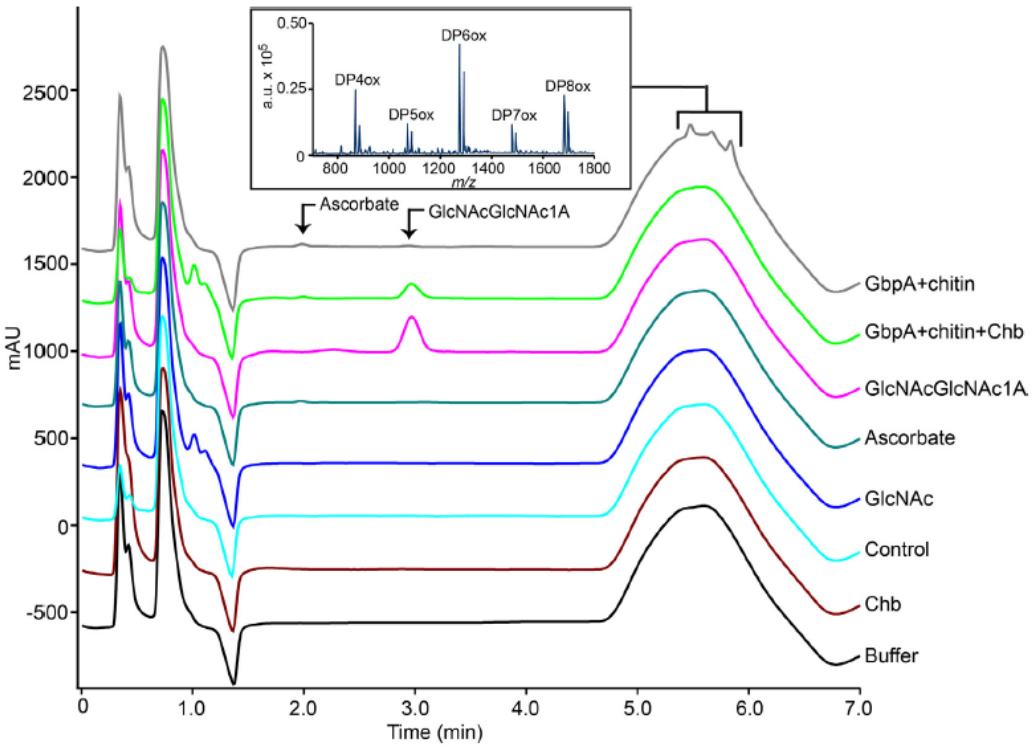

Figure 7. Analysis of LPMO products released from chitin-active LPMO buffered in 50 mM Bis-Tris, pH 6.8, and ascorbic acid. MS: each chito-oligosaccharide is identified by one peak. After treatment with chitobiase (Chb) only one peak (chitobionic acid) is visible. (22)

1.3 Cellobiose dehydrogenase

Cellobiose dehydrogenase is a ubiquitously distributed enzyme in wood degrading fungi. CDH acts as electron donor and was shown to activate LPMO. CDH is active on soluble β-(1,4) interlinked saccharides and has highest catalytic efficiencies for cellobiose and lactose. (4)

1.3.1 Structure

CDH has a two-domain architecture comprising an electron transferring cytochrome *b* domain (CYT) and a sugar oxidizing flavodehydrogenase (DH) domain. The domains are connected by a linker peptide.

The CYT domain has a β-sandwich topology with a central hydrophobic heme *b* binding pocket. It`s iron is hexa-coordinated by Met and His. (23)

DH is a member of the glucose-methanol-choline family of sugar oxidoreductases and contains a non-covalently bound FAD in the active site. (24) DH has two subdomains, one responsible to bind FAD and one substrate binding domain.(4)

1.3.2 Electron transfer

CDHs flexible two-domain structure empowers it to transfer electrons to external redox-active compounds. The cytochrome domain is responsible for the interaction with external electron acceptors. (25) It is believed that there is a sequential electron transfer chain from FAD to CYT, as the oxidative potential of heme *b* is higher than that of the FAD. The redox potential denotes the tendency of a chemical species to acquire electrons. (4)

1.4 Cellobiose dehydrogenase for improved H_2O_2 production

*Mt*CDH *Oxy*$^+$ is a CDH variant and has an increased oxygen reactivity when compared to the wild-type enzyme and thus produces more H_2O_2 than the wild-type enzyme.

1.5 Activation of *Nc*LPMO9C

Activity of LPMO depends on reduction by an external electron donor. This donor could be either a small molecule reductant like ascorbic acid, gallic acid, low molecular weight lignin (20), or an electron transferring enzyme, like CDH.
Activators can be divided in three main groups: CDHs, plant or fungal phenols and regeneration of these via other secreted GMC oxidoreductases.(20)

1.5.1 Interaction CDH and LPMO

A first indicator that CDH is an activator for LPMO is the frequent co-expression of both enzymes during lignocellulose degradation. (19) Moreover, *cdh* and *lpmo* genes show a high overlap in many fungal genomes. (26) In 2011, the electron transferring properties of CDH were first connected to the enigmatic activity of LPMO using biochemical methods. (27) It is now established that CDH transfers electrons via its CYT-domain to reduce the active-site copper of LPMO to initiate cellulose attack. (20) Kracher et. al (20) used rapid spectroscopy experiments to demonstrate fast electron transfer rates between CDH and LPMO, which are dependent on pH. The structures of all enzymes used can be seen in Figure 8.

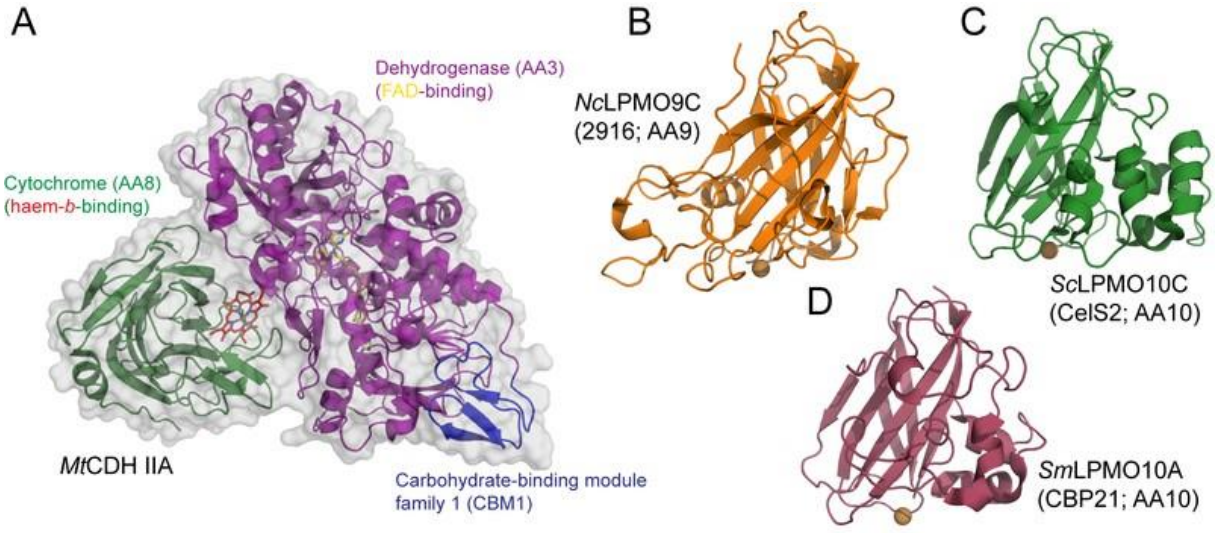

Figure 8. Structures of used enzymes in this work. CDHIIA from *Myriococcum thermophilum* (*Mt*CDH; red: heme; blue: family 1 carbohydrate binding module; yellow: FAD; purple: DH domain; green: cytochrome domain) *Nc*LPMO9c (cellulose active C4 oxidizing enzyme), *Sc*LPMO10C (cellulose active C1 oxidizing enzyme), CBP21 = *Sm*LPMO10A (chitin active C1 oxidizing enzyme).

1.6 Aims of the study

The aim of this study was to elucidate catalytic rates for different LPMOs, while focusing on the efficient activation of LPMOs. This information is important to improve product formation from insoluble polysaccharides leading to higher yields in plant biomass degradation.

This goal was divided into two major topics. To be able to follow real-time LPMO activation an electrochemical method based on hydrogen peroxide reduction should be established.
In the second part, product formation should be tracked using HPLC and MS to compare different activation possibilities of LPMO. Four different CDHs (*Mt*CDH IIA, *Mt*DH IIA, *Mt*CDH Oxy^+ and *Mt*DH Oxy^+) were tested as reductants for two different LPMOs (*Nc*LPMO9C and CBP21).

2 Materials and Methods

All chemicals used during this work were of analytical grade and highest purity available and were purchased from Fluka (Vienna, Austria), Sigma-Aldrich (Vienna, Austria), Merck (Darmstadt, Germany) or Roth (Karlsruhe, Germany. All aqueous solutions were prepared with deionized reversed osmosis water (conductivity < 0.06 µS cm^{-1}).

2.1.1 Buffers

Phosphate buffer, 50 mM, pH 6.0

KH_2PO_4 and K_2HPO_4 titrated with NaOH

Bis-Tris buffer

2,2-Bis(hydroxymethyl)-2,2',2"-nitrilotriethanol titrated with HCl

Mass spectrometry buffer

$CH_3COONa.3\times H_2O$ 2.41 g L^{-1} and CH_3CO_2H 174 µL L^{-1}

2.1.2 Enzymes

Native NcLPMO9C and CDHs from the ascomycetous fungus *Myriococcum thermophilum* were recombinant gene products produced in the yeast *Pichia pastoris.* The purified enzymes were provided by the Department of Food Science and Technology, University of Natural Resources and Life Sciences, Vienna, Austria. The purified CBP21 and the chitobiase were provided by the Department of Biotechnology of the Norwegian University of Life Sciences, Ås, Norway.

Table 1. List of enzymes used during the project.

Enzyme	Application	Full name
*Mt*CDH IIA	Activation of LPMO	*Myriococcum thermophilum* cellobiose dehydogenase
*Mt*DH IIA	Activation of LPMO	*Myriococcum thermophilum* FAD-dehydogenase
*Mt*CDH Oxy^+	Activation of LPMO	*Myriococcum thermophilum* cellobiose dehydrogenase mutant; oxygen consumption enhanced
*Mt*DH Oxy^+	Activation of LPMO	*Myriococcum thermophilum*

		FAD-dehydrogenase mutant; oxygen consumption enhanced
*Nc*LPMO9c	Kinetic measurements	Lytic polysaccharide monooxygenase *9C* from *Neurospora crassa*
CBP21	Kinetic measurements	Lytic polysaccharide monooxygenase *10A* from *Serratia marcescens*
Chit B	Quantification CBP21 products	Chitobiase
*Pc*P2O	Activation of LPMO	*Phanerochaete chrsosporium* pyranose 2 oxidase
Cels2	Degradation of CBP21 products to quantify them	Lytic polysaccharide monooxygenase *10C Streptomyces coelicolor*

2.2 Methods

2.2.1 Electrochemistry

To follow the reaction kinetics of LPMO an electrochemical setup was used to measure the H_2O_2 consumption during oxidative substrate oxidation. This setup included a potentiometer, a motor controller, a water bath and three electrodes, known as counter electrode, working electrode and reference electrode. The setup can be seen in Figure 9.

Electrochemistry is the study of chemical processes that cause electrons to move. These reactions are known as redox reactions. (28) Occurrence of redox-reactions causes the release or consumption of electrons, which can be detected. In the herein used setup, the oxidation of H_2O_2 at a platinum electrode surface was measured. The free energy released in this reaction occurs as electrical energy, which can be measured and quantified as electrical current. (29)

The H_2O_2 oxidation on a platinum electrode is a diffusion limited reaction. The applied negative potential determines the oxidized platinum surface of the electrode by reducing the electrode. (30)

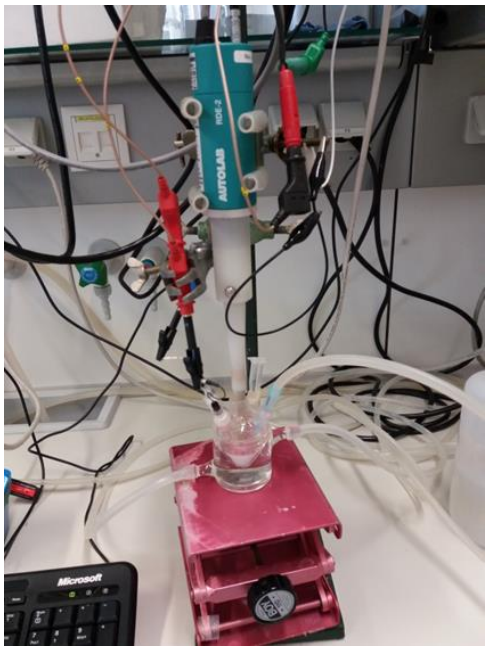

Figure 9. Electrochemical setup: electrochemical cell, in the middle of the cell is the counter elctrode. To the left the are the reference and the working electode. Through the blue tip nitrogen is supplied. Temperature is controlled via water bath.

2.2.1.1 Working electrode

The working electrode takes part in the reaction of the electrochemical system. Usually it is made out of inert material, like platinum. (31)
Before usage, the electrode was rinsed with deionized water. To obtain a homogenous surface, the electrode was polished using wet sand paper (P600) by drawing "eights" onto the paper. It was important to twist the electrode slowly to achieve equal polishing. After flushing with water, the electrode was treated with a finer micro cloth to obtain a smoother surface. This was done using Masterprep solution (0.05 µM fine dispersed particles, aluminium oxide; Buehler MasterPrep). To remove all particles the electrode was washed with deionized water and sonicated for 5 min in highly purified osmotic water.

A platinum micro-electrode was used because it readily reacts with H_2O_2. Such a small electrode prevents excessive consumption of the analyte (H_2O_2) in experiments with a long running time. A disadvantage of using micro-electrodes is the low signal outputs, which were typically in the nanoampere range. The system was very sensitive and had a detection limit of less than a view nanoamperes.

2.2.1.2 Reference electrode

The reference electrode has a stable and known potential which can be used as a reference point in the electrochemical system, since the potential needs to be highly stable. This can be achieved by employing a redox system in which the concentration of each chemical compound is kept at a constant concentration. In addition, the current-flow through the electrode is kept close to zero. (31)
Here, a silver/silver-chloride reference electrode was used, which was stored in 3 M KCl.

2.2.1.3 Counter electrode

A platinum electrode was used as counter electrode. This electrode was approximately 5 cm long and had a diameter of 1 mm. It is known as auxiliary electrode as well. It was necessary to close the current circuit in the electrochemical cell which does not take part in the reaction. As the current flows between the working- and the counter-electrode, the total surface of the auxiliary electrode has to be high enough to make sure it will not be a limiting factor in the kinetics of the electrochemical reaction. (31)

This electrode setup was combined with a motor controller to obtain a rotating disc electrode. Spinning of the electrode provided an optimal homogenization in the cell. In addition, a plastic piece (5 $\times$ 3 $\times$ 2 mm) was fixed with parafilm at the tip of the electrode to increase its stirring efficiency as seen in Figure 10.

Figure 10. Counter-electrode: the electrode was used as rotating disc electrode. A plastic piece fixed with parafilm was used as stirrer to increase mass-transfer in the cell.

2.2.1.4 Procedure

The experiments were performed using an electrochemical cell. In the cell the reference and working electrodes were fixed with parafilm. In the third vent nitrogen bubbling was supplied through a pipette tip. The vent in the middle was used to insert the rotating disc counter electrode. The cell was surrounded by a double jacket connected to a temperate water bath which allowed maintaining a defined temperature throughout the experiment.

Nitrogen bubbling was maintained throughout all experiments and the water bath was set to 30 °C. The motor controller was set to 500 rpm. This empirically determined value provided optimal mixing while preventing unnecessarily high shear forces, which might harm enzymes in combination with nitrogen sparging. To equilibrate the system this setup as seen in Figure 11 was ran for 10 min before starting the experiment.

Figure 11. Setup of electrochemical measurments. (A) Water bath (temperature was set to 30 °C). (B) The motor controller and (C) electrochemical cell with attached electrodes.

2.2.1.5 Software Nova 1:11

The software NOVA 1.11 (Metrohm, Autolab) was used to control the system as seen in Figure12.

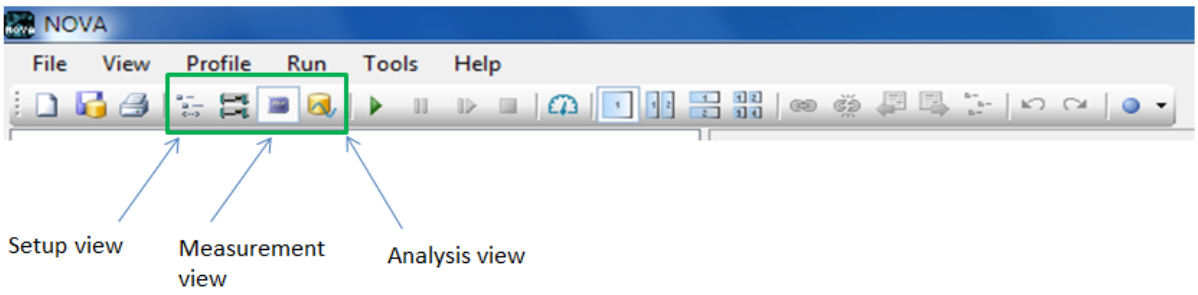

Figure 12. Software Nova 1.11. The icons "Setup view", "Measurement view" and "Analysis view" used for electrochemical measurement and data evaluation.

In the icon setup view it was possible to name all experiments. The potential was set to 0.400 Volts. The current was measured in Ampere over time. The interval time, which denotes the time within two consecutive reading points, was set to 1 data point per second.

Each measurement was started and monitored online using the symbol called "Measurement view". Signals were overlaid in "Analysis view".

2.2.2 High Pressure Liquid Chromatography (HPLC)

2.2.2.1 Systems used

Product analysis was done by HPLC using a DIONEX Ultimate 3000 system (all equipment from Thermo Scientific), which was used to analyse the oligosaccharide products of cellulose-active LPMOs at a total running time of 50 min per run. Alternatively, DIONEX ICS-5000$^+$ or 3000$^+$ (Thermo Scientic) systems were used to analyse the products of chitin-active LPMOs at a total running time 6 min per run.

2.2.2.2 HPAEC principle

HPAEC is the abbreviation of high performance anion exchange chromatography which is used to separate molecules based on their negative net surface charge. Three eluents were necessary to analyse oligosaccharides: 0.1 M NaOH, 1 M sodium acetate and highly purified water. Samples were separated at a flow rate of 0.25 mL/min. An isocratic gradient was applied and a pressure of approximately 1200 psi was used.

2.2.3 Mass spectrometry

2.2.3.1 Sample preparation

Samples were diluted in 50 mM Bis-Tris buffer, pH 6.8. Two µL of 9 % dihydroxybenzoic acid (3.5 mg in 117 µL acetonitril and 272 µL water) were pipetted on an MTP 384 ground steel plate and mixed with 1 µL of the sample solution. After drying with a hair dryer the plate was fixed into a dedicated brace and inserted in the MALDI-TOF.(11)

MALDI-TOF

MALDI is the abbreviation for "Matrix Assisted Laser Desorption/Ionization". Samples are mixed with a matrix molecule as described above. The matrix absorbs ultraviolet light and converts it to heat causing the sample to evaporate. Charged ions in different sizes are generated. Ions with smaller mass-to-charge ratios and highly charged ions move faster to the detector, which means that the time of flight differs for different mass-to-charge ratios. (32)
A system from Bruker Daltonics, Bremen, Germany was used in positive mode with an acceleration voltage of 25 kV, a reflector voltage of 26 kV and pulsed ion extraction of 40 ns. 300 shots were applied on each spot in the mass-to-charge range from 300 to 3000, with the lowest laser energy necessary to obtain a sufficient signal-to-noise ratio. Data were analysed using the FlexControle 3.3 software (Bruker). (11)

2.2.4 Amplex Red assay

The Amplex Red assay was used to quantify the enzymatic H_2O_2 production. It is based on a side reaction of LPMO,seen in Figure 13 which occurs in the absence of the natural substrate cellulose. Upon reductive activation of the type-2 copper in LPMO using ascorbic acid or CDH in combination with cellobiose, oxygen is reduced at the LPMO active site. H_2O_2 is released and detected by the horseradish peroxidise-coupled conversion of Amplex Red to the fluorescent Reorufin. By adding different concentrations of H_2O_2 producing enzymes, the kinetics of H_2O_2 formation could be analysed.

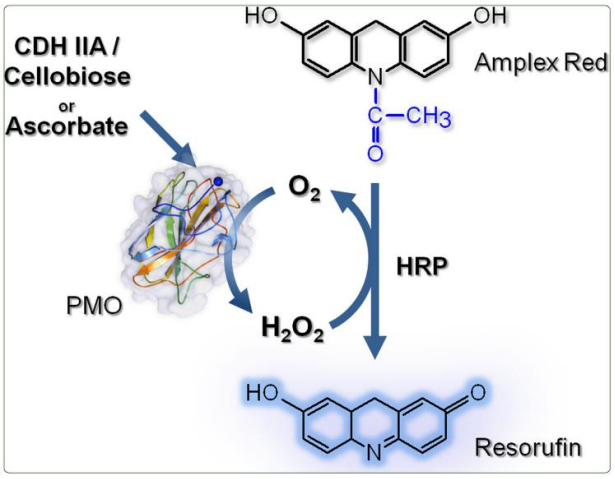

Figure 13. Amplex Red Assay. Measurement of H_2O_2.

2.3 Results and Discussion

2.3.1 Reaction kinetics

2.3.1.1 Influence of oxygen vs. nitrogen in electrochemistry

Oxygen, which can be reduced at the electrode surface, is a potential interfering factor during the electrochemical measurements. To assess the effect of oxygen on the amperometric signal, an experiment was carried out in which the cell was bubbled with nitrogen (anoxic conditions) and oxygen while monitoring the buffer baseline.

In the beginning of the reaction (Figure 13, Phase 1), neither nitrogen nor oxygen was added during the measurement. At about 400 sec (Figure 13, Phase 2) very low nitrogen bubbling was applied, which lead to a temporal decrease in signal intensity. At the applied low nitrogen intake, the amperometric signal started to increase again. In Phase 3 the nitrogen bubbling was increased, and this led to an instant decrease in signal intensity. After increasing the nitrogen supply further, the buffer line was reached (Phase 4") and led to a stable signal and low background noise.

After stopping the nitrogen supply, the signal increased gently in Phase 5 followed by a huge increase upon low oxygen bubbling. To complete the experiment oxygen intake was increased to a maximum supply which led to high background noise, a very unstable system and a background noise. The lowest signal-to-noise ratio and the most stable signal were achieved by moderately

adding nitrogen to the electrochemical cell. This setup was used in all following experiments.

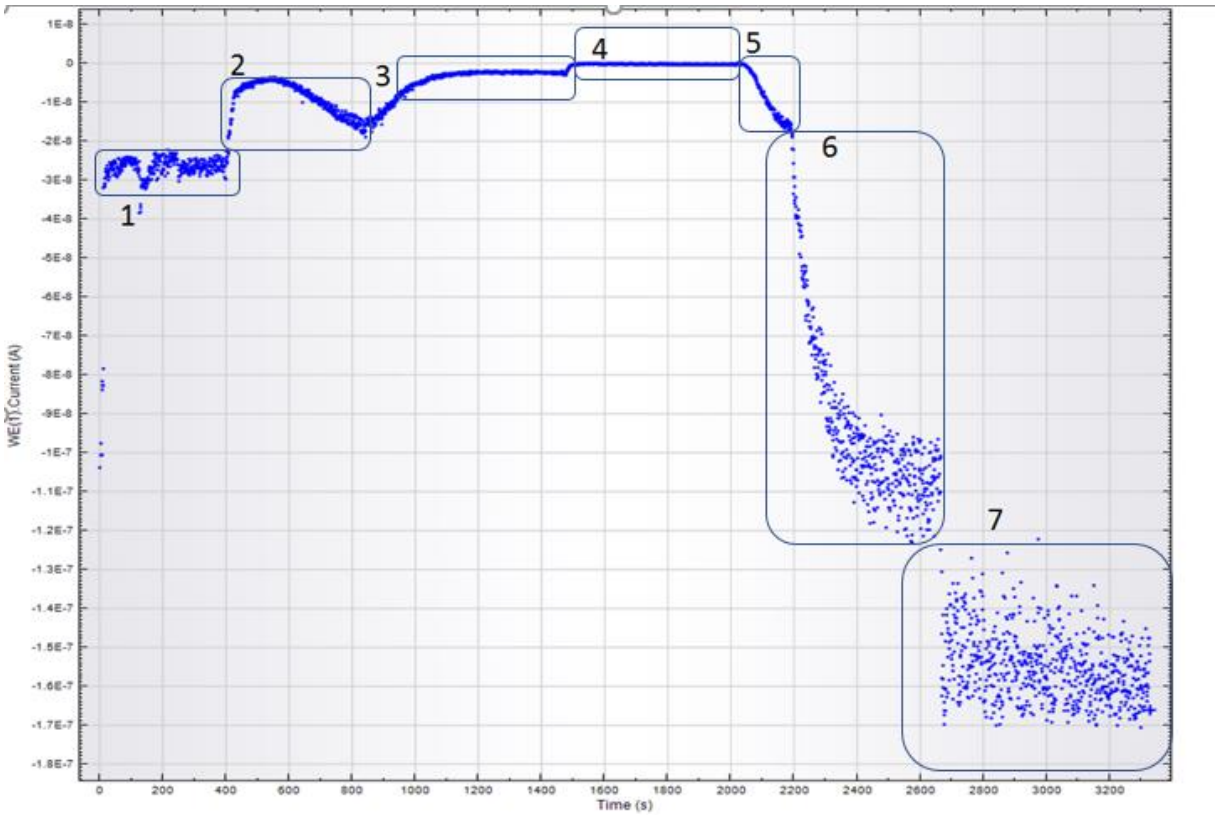

Figure 14. Signal in response to different gas bubbling rates. See text for explanation.

2.3.1.2 Finding the optimal voltage of the working electrode

To determine a voltage range which allowed to reliably quantifying the analyte, cyclic voltammetry was performed. This is an electrochemical method where the potential is swept within a range of potentials. The current is plotted against the applied potential. This cyclic measurement was performed between -600 and 600 mV. The first run was performed in presence of 6.6 mg/mL PASC (Figure 14, blue trace) followed by addition of 100 µM H_2O_2 (Figure 15, green traces). To be able to see the signal caused by H_2O_2, a potential of -400 mV was chosen. This experiment was performed under anaerobic conditions, which was achieved by constant bubbling with nitrogen. The reason for the decrease in the lower two green traces in the range of -500 and 100 mV was a stop in nitrogen bubbling, which led to oxygen intake into the cell which caused a shift in the signal.

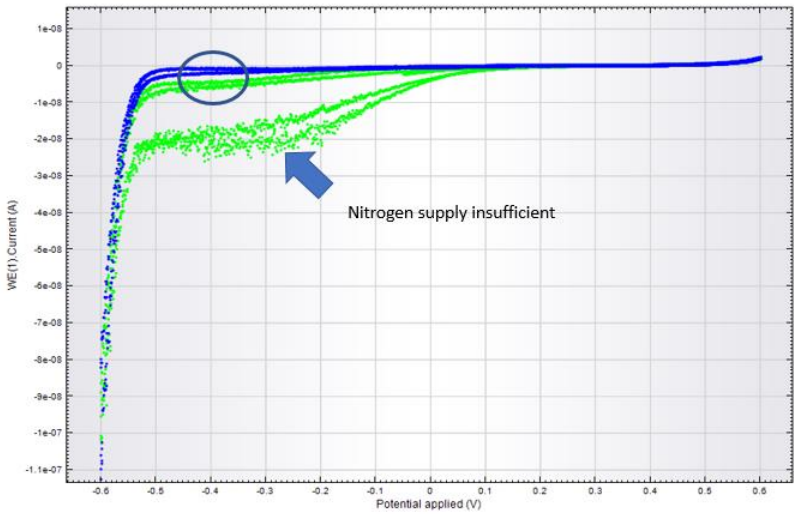

Figure 15. **Cyclic voltammetry** (-600 mV-600 mV). blue lines: measurement of PASC; green lines: measurement of PASC and H_2O_2.

2.3.1.3 Calibration with H_2O_2

To verify that H_2O_2 can be quantitatively measured, a calibration curve for peroxide was generated. Upon adding 10, 20, 30 and 40 µM H_2O_2 to PASC, a final concentration of 100 µM was achieved. For each addition the amperometric output after stabilization of the signal was plotted against the applied H_2O_2 concentration. The linearity of the calibration curves confirmed that H_2O_2 could be measured quantitatively.

After addition of 100 µM H_2O_2, 1.25 µM LPMO was added to the reaction. To initiate LPMO activity, 20 µM ascorbic acid was added after 930 sec to supply electrons to the LPMO active site (Figure 16). LPMO alone did not have an effect on the signal. The time-dependent consumption of H_2O_2 during the reaction could be followed via the decrease of the amperometric signal, which eventually stopped at the buffer level at about 0 nA. With reaching the baseline, 100 µM H_2O_2 were consumed. Based on these data it can be concluded that H_2O_2 is consumed during the reaction.

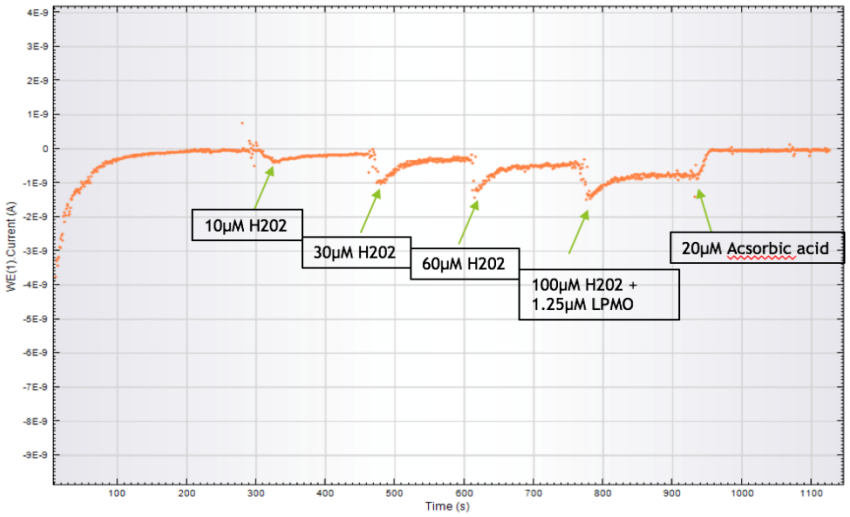

Figure 16. Calibration with H_2O_2 in PASC. At 320 sec 10 µM hydrogen was added, at 480 s 20 µM, at 600 s 30 µM and at 780 s 40 µM and 1.25 µM LPMO. At 940 s 20 µM ascorbic acidascorbate was added.

The H_2O_2 calibration was repeated in buffer without addition of PASC. (Figure 17) After adding 1.25 µMLPMO and ascorbic acidascorbate the signal remained at a constant level, which demonstrates that the H_2O_2 was not consumed. This indicates that the substrate PASC is required as electron acceptor of the enzyme.

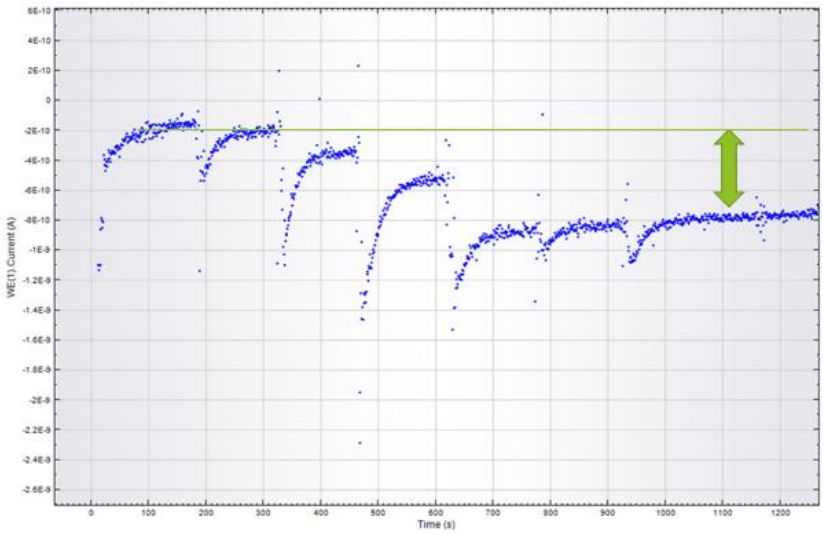

Figure 17. Calibration with H_2O_2 in 50 mM phosphate buffer. the green line indicates the buffer level from 0 s to 700 sec calibration (same procedure as figure 6) After adding 20 µM ascorbic acid at 790 sec and at 950 sec signal did not return to the buffer level.

2.3.1.4 Testing quantitative reproducibility

After calibration and addition of LPMO as described above, 2.5 µM ascorbic acid (final concentration) was added after 1000 sec followed by 7 more additions every 200 sec as shown in Figure 18 (red line). Traces in blue indicate a reaction performed under the same conditions, except that 5 µM of ascorbic acid were added every 400 sec. The system leveled off at the same level for both experiments (addition of two times 2.5 µM or once 5 µM).

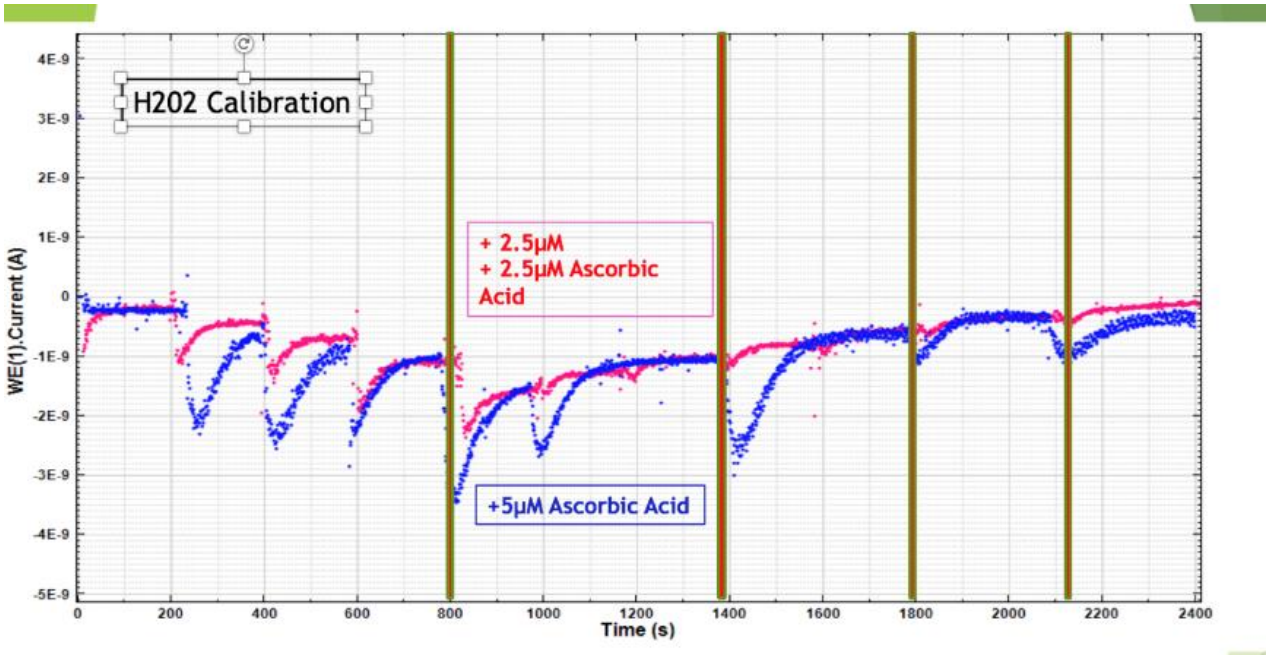

Figure 18. Quantitative reproducibility of the system using platinum microelectrode to quantify H_2O_2.

2.3.1.5 Ascorbic acid-dependence of the H_2O_2 consumption and repeatability of catalytic cycles

To elucidate whether the changes in signal intensity after adding ascorbic acidwere caused by the enzyme, or are due to the system which needs time to achieve equilibrium conditions, two experiments were performed. In the first experiment, (Figure 19, orange traces), 1.25 µM LPMO and 100 µM H_2O_2 were added at 220 sec. At 500 sec, 15 µM ascorbic acid were injected, which lead to a total consumption of H_2O_2 within 600 sec. After adding another 15 µM ascorbic acid at 900 sec, the signal did not reach the basis level anymore, which indicates that there was still H_2O_2 left. To make sure that there was enough electron donor

available, again 15 µM of ascorbic acid were added. However, the signal remained at the same level, which can be due to inactivation of the enzyme caused by to high amounts of H_2O_2, or it could indicate inhibition of the LPMO. After adding H_2O_2 a third time, ascorbic acid did not lead to an increase in signal anymore.

The second experiment was performed under the same conditions, but in absence of LPMO (Figure 19, pink trace). The decreases after addition of ascorbic acid were lower, which excludes the disturbance of the electrochemical setup through adding ascorbic acid as a cause for the decreases of the signal. This confirms that the signal changes observed in presence of LPMO were caused by an enzymatic turnover of peroxide.

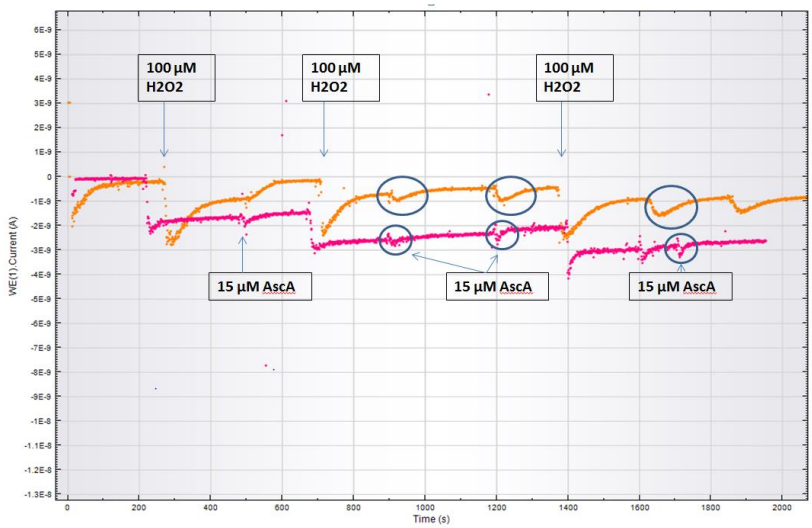

Figure 19. Signal decreases after adding ascorbic acid and testing repeatability of catalytical cycles. In orange: PASC and 1.25 µM LPMO was in the cell. At 220, 700 and 1400 sec addition of H_2O_2, at 500, 900, 1200 and 1700 sec addition of 15 µM ascorbic acid. In pink: same setup as in orange except any LPMO.

2.3.1.6 Repeatability

The following experiment was repeated four times at 30 °C to test the reproducibility of the measurement. In a total volume of 4 mL buffer solution containing 6.6 mg/mL PASC a H_2O_2 calibration curve was generated as described in section 2.3.1.3. After 800 sec of equilibration, 1.25 µM LPMO were added to the cell followed by sequential addition of 2.5 µM ascorbic acid every 200 sec. Amperometric signals shown in Figure 20 (blue and purple traces) illustrate that

approx. 10 µM ascorbic acid were necessary to deplete 100 µM of H_2O_2. Thus, the stoichiometry of the reaction was approx. 1:10 (ascorbic acid: H_2O_2) in this experiment. In comparison, the stoichiometry was 1:6.6 when 15 µM ascorbic acid were used together with the same amount of H_2O_2 (Figure 20, red and green traces). There is a significant deviation on signal intensity between different experiments can be explained by the very low signals measured in the nA range. Therefore, it was essential to generate a calibration curve for every individual run.

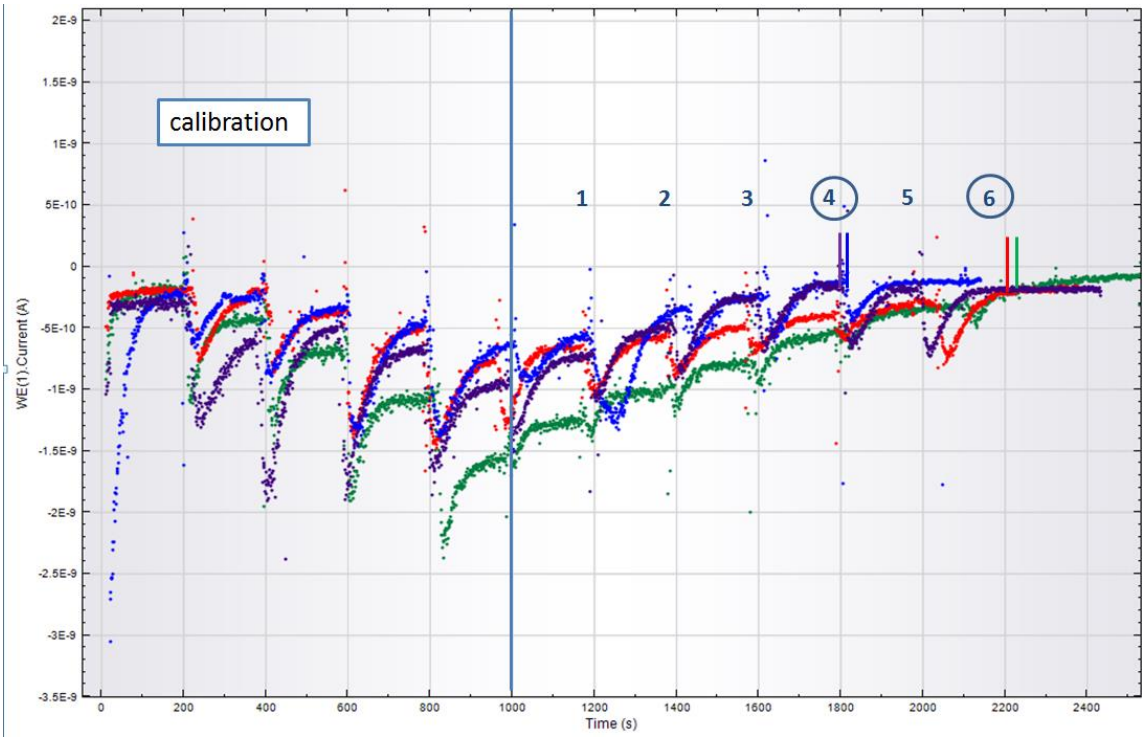

Figure 20. Repeatability at 30°C. each color represents one experiment repeated under same conditions. The numbers are equal to the number of 2.5 µM ascorbic acid additions.

2.3.1.7 Temperature dependence of H_2O_2 consumption

In the following experiment the impact of temperature on the peroxide turnover was tested. All reactions started with a H_2O_2 calibration curve from 220 to 800 sec, followed by addition of 1.25 µM LPMO and stepwise additions of 2.5 µM ascorbic acid every 200 sec. The same experiment was performed at 20°C (green), 30°C (orange), 40°C (pink) and 50°C.(blue) The electrochemical cell had a total volume of 4 mL. (Figure 21) All experiments were performed as

duplicates. The observed high deviation in these experiments is due to the low currents measured, which were close to the detection limit in the sub-nanoampere range.

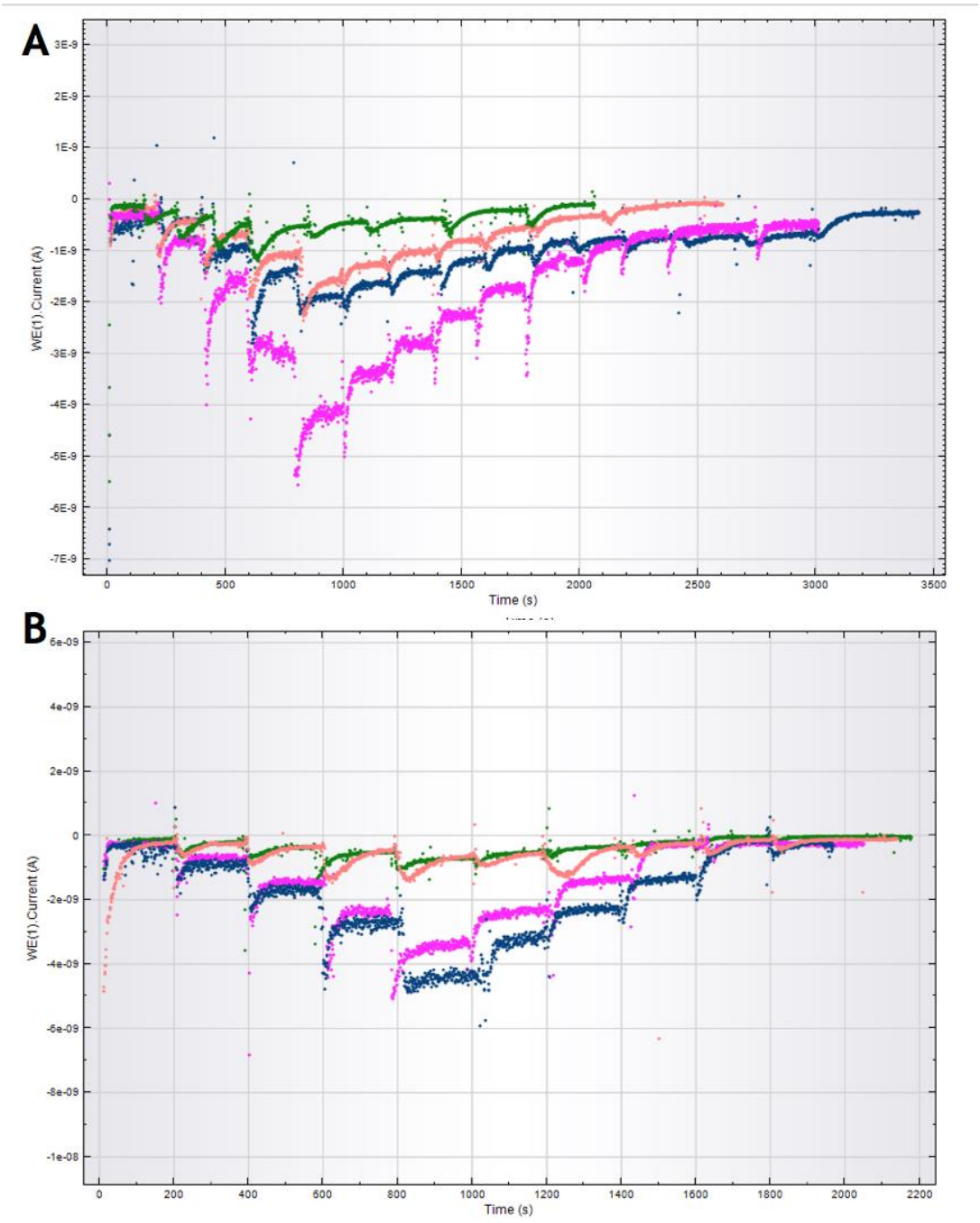

Figure 21. Ascorbic acid consumption at different Temperatures (green = 20 °C, peach = 30°C pink = 40°C, blue = 50°C) (A) first setup (B) second setup.

After adding H_2O_2 to the reaction, the amperometric signals levelled off at a constant level within one minute. H_2O_2 calibration curves generated at different temperatures are shown in Figure 22.

It seems like higher temperature leads to higher signals including higher background noise. Concluding from Figure 21 more ascorbic acid is necessary to return to the buffer level with increasing temperature this means reaction time gets longer which is untypical according to the Arrhenius equation. These results are not significant. Reaction velocity is faster than expected for an enzyme catalyzed reaction, within sec H_2O_2 is consumed. One important factor is the response time of the instrument which is not known concluding we cannot reliably measure very fast reactions.

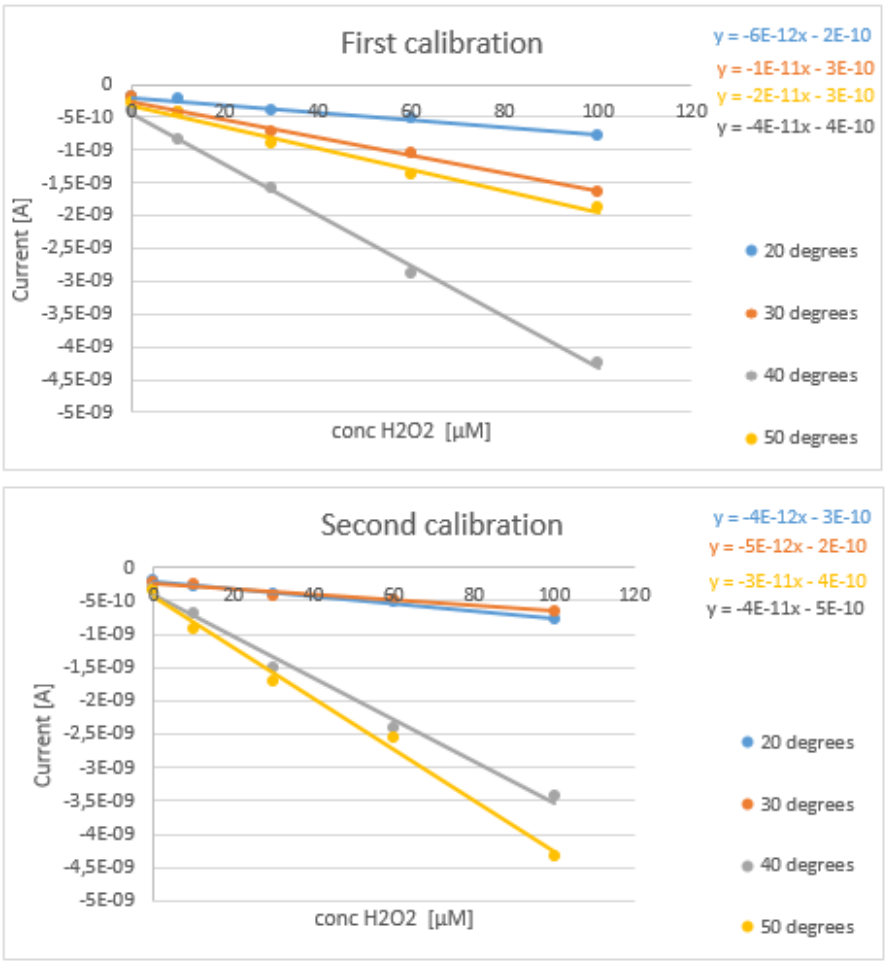

Figure 22. H_2O_2 **calibration.** duplicate. measured signal in A versus concentration of H_2O_2in the cell. 50 degrees (A blue): After adding 10 µM H_2O_2 the signal levels up at -9,3964 E-10 A.

Table 2. Ascorbic acid consumption to neutralize 100 µM H_2O_2 at 20, 30, 40, 50 °C and repetitions.

	20 °C		30°C			40°C		50 °C	
	I	II	I	II	III	I	II	I	II
Ascorbic acid added	15.0	17.5	15.0	7.5	7.5	17.2	7.5	19.2	10.0
H_2O_2 consumed at each addition of 2.5 µM Ascorbic acid									
1	26.0	24.4	2.1	26.4	32.9	26.6	35.0	32.0	33.6
2	9.7	11.5	19.5	43.1	54.2	13.4	32.6	11.6	19.2
3	13.8	25.3	29.5	30.5	12.9	15.9	32.4	12.1	24.1
4	18.2	24.3	20.1			9.6		11.3	23.1
5	16.4		24.0			15.8		6.1	
6	16.0		4.7			6.1		5.1	
7						6.6			
mean	16.7	21.4	16.7	33.3	33.3	13.4	33.3	13.0	25.0
stoichiometry	6.7	5.7	6.7	13.3	13.3	5.8	13.3	5.2	10.0

µmol H_2O_2 consumed/µmol Ascorbic acid			
20 °C	7.4	±	2.3
30 °C	12.5	±	4.2
40 °C	9.1	±	3.8
50 °C	8.4	±	3.3

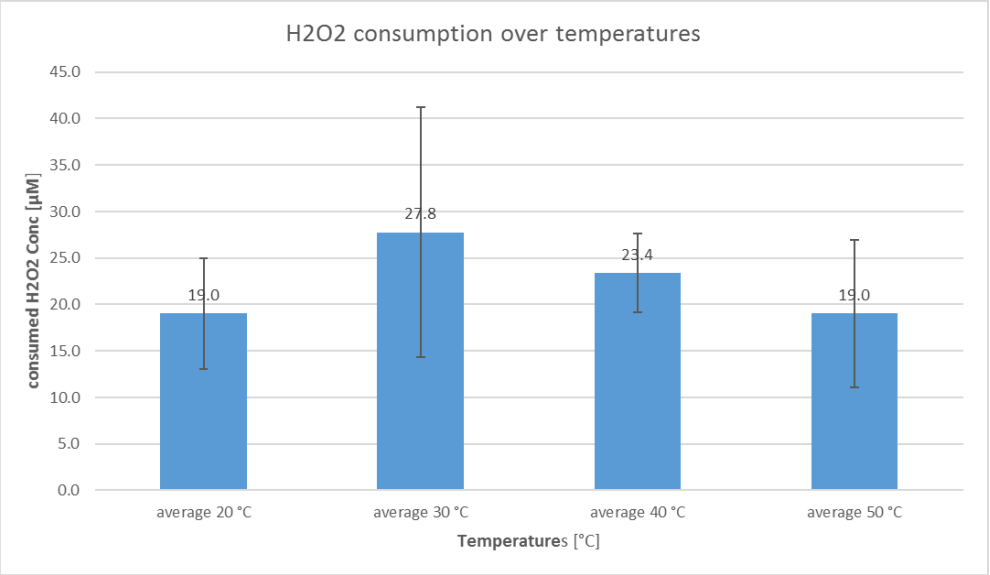

Figure 23. H_2O_2 consumption [µM] per 2.5 µM ascorbic acid at 20, 30, 40 and 50 °C.

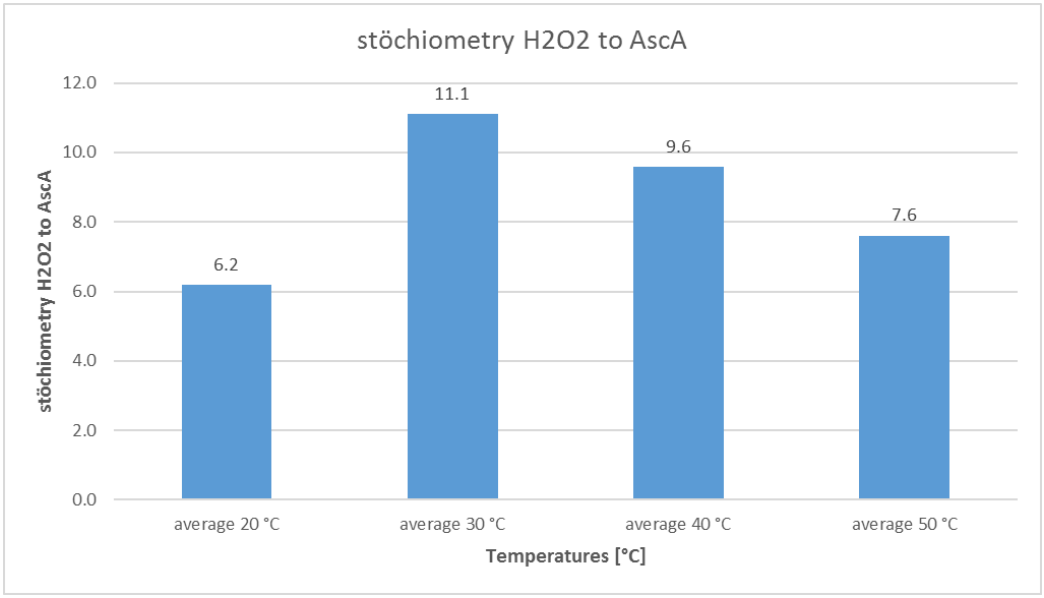

Figure 24. Stoichiometry H_2O_2 to ascorbic acid at 20, 30, 40 and 50 °C.

2.3.1.8 Calculation the k_{cat} of LPMO at 30 °C

Figure 25 shows a typical plot of the H_2O_2 concentration vs. current output at 30°C. The slope of the calibration curve denotes the current change for each µM of H_2O_2, which was about -1^{-11} A.

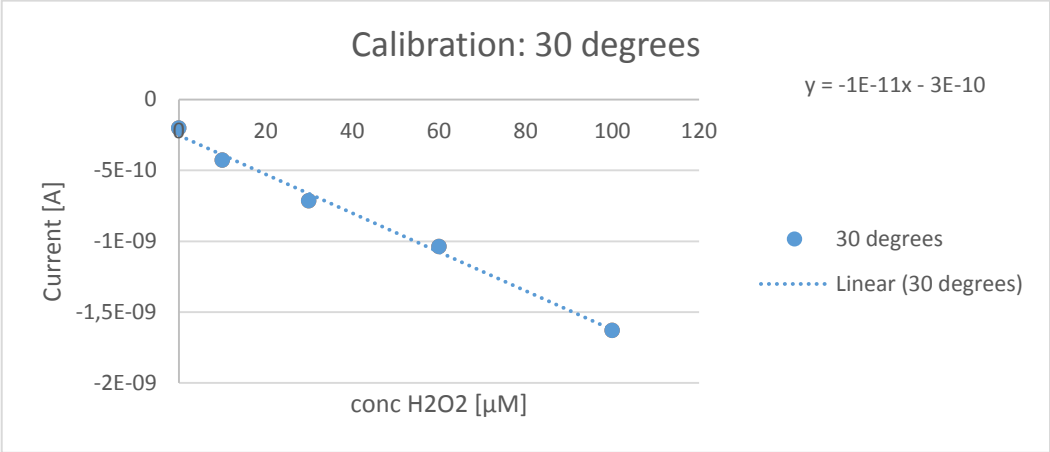

Figure 25. calibration at 30 degrees.

After addition of H_2O_2, 1.25 µM LPMO and 2.5 µM ascorbic acid were added to the cell. Upon each addition of ascorbic acid, a linear increase in signal was observed, which can be seen in Figure 26. Using the observed slopes from the initial decrease of the signal, apparent catalytic rates were calculated for each addition of ascorbic acid.

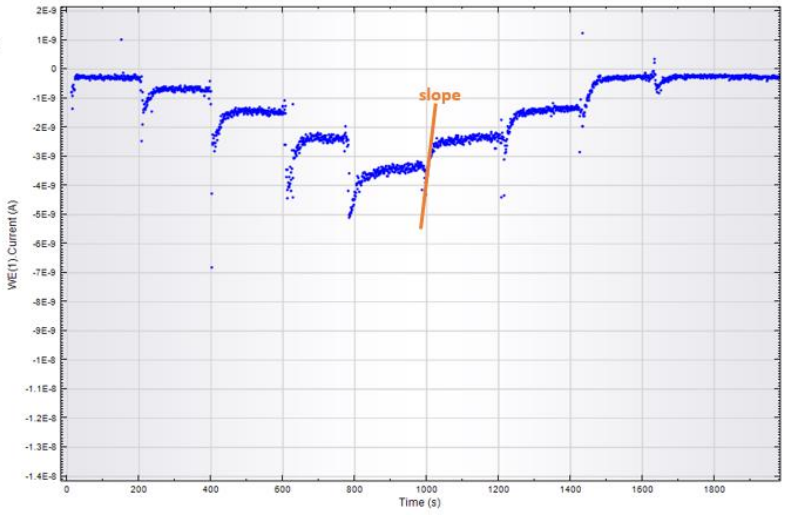

Figure 26. electrochemical slope to calculate rates.

Table 3. Calculation of k_{cat} for LPMO using ascorbic acid as electron donor and H_2O_2 as the co-substrate.

Slope (A/s)	Slope (A/min)	µmol/min	s-1
5.0E-12	3.0E-10	1.9E+04	250
5.9E-12	3.5E-10	2.2E+04	290
4.5E-12	2.7E-10	1.7E+04	220
5.1E-12	3.1E-10	1.9E+04	250
2.5E-12	1.5E-10	9.4E+03	130
3.9E-12	2.3E-10	1.4E+04	190

2.3.1.9 Interaction CDH and LPMO: Calculation of rates

To test if CDH can act as an electron donor and H_2O_2supplier for LPMO, a reaction was set up containing 3.5 mL 6.6 mg/mL PASC, 5 mM lactose and 100 µM H_2O_2. After adding either CDH or LPMO there was no current change, which means that there was no reaction taking place. When the second enzyme (CDH) was added, an immediate reaction occurred. CDH transfers electrons to LPMO, which is reduced and oxidizes the co-substrate H_2O_2. The kinetic reaction can be seen in Figure 27. There was no difference when either LPMO or CDH was added first, which is visible in the blue and green traces shown in Figure 27. The grey trace is a buffer control in absence of PASC and enzymes.

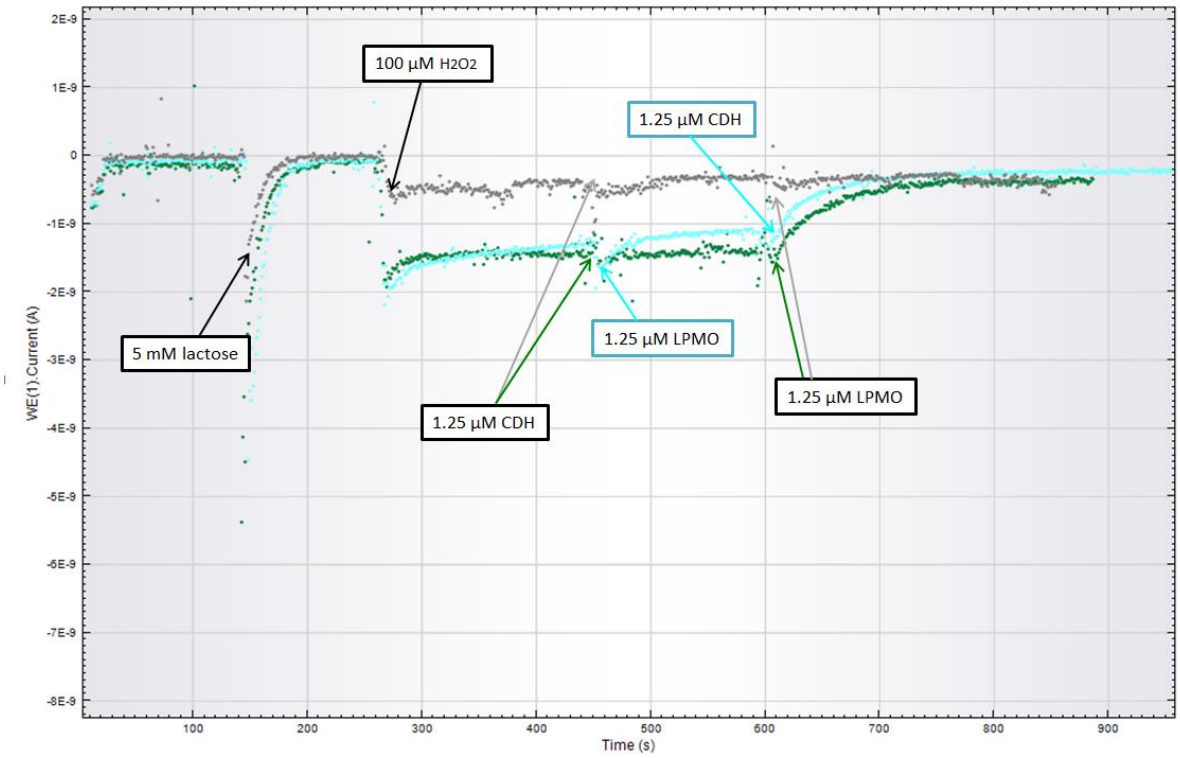

Figure 27. interaction CDH and LPMO. Green: addition of 5 mM lactose, 100 µM H_2O_2 1.25 µM CDH and 1.25 µM LPMO. blue: 5 mM lactose, 100 µM H_2O_2, 1.25 µM LPMO, 1.25 µM CDH. CDH provides electrons to LPMO. LPMO oxidizes H_2O_2 to H_2O.

2.3.1.10 Varying ratio between LPMO and CDH

To find out which ratio between LPMO and CDH is necessary to provide enough electrons to start the reaction, the same setup as previously described (Section 2.2.1) was performed. However, the amount of CDH was varied in these experiments. After adding lactose to PASC and sequentially adding H_2O_2, CDH was added in different concentrations ranging from 0.08 µM (ratio CDH:LPMO = 1:16) to 1.25 µM (ratio 1:1). The concentration of LPMO was kept at 1.25 µM throughout all experiments. With decreasing amounts of CDH, the reaction rate decreased. Color code for Figure 28 and 29 is explained in Table 4.

Table 4. explaining color code different ratios LPMO to CDH.

color	Concentration of CDH [µM]	Ratio LPMO to CDH
dark green	1.25	1
blue	0.63	2
purple	0.31	4
pink	0.16	8
Light green	0.08	16

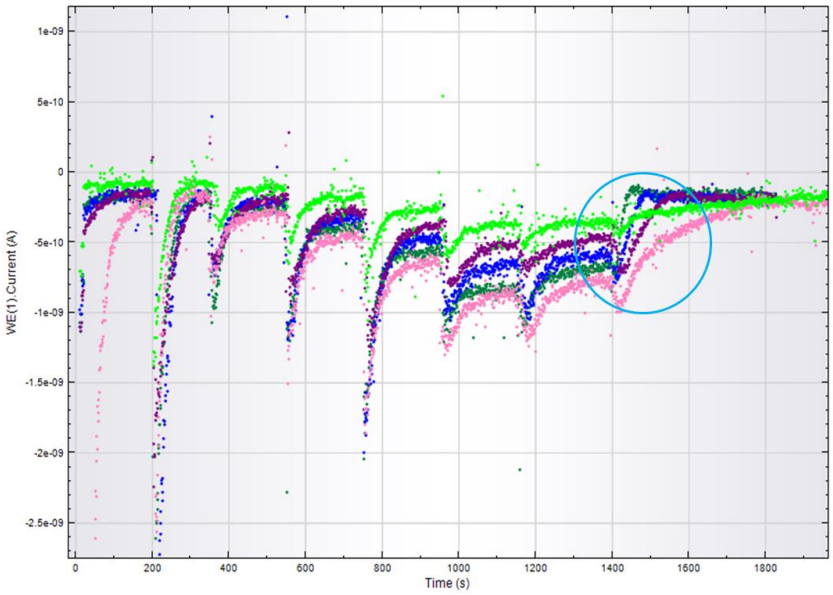

Figure 28. First experimental series varying CDH concentration in correlation to LPMO. The color code is explained in Table 4.

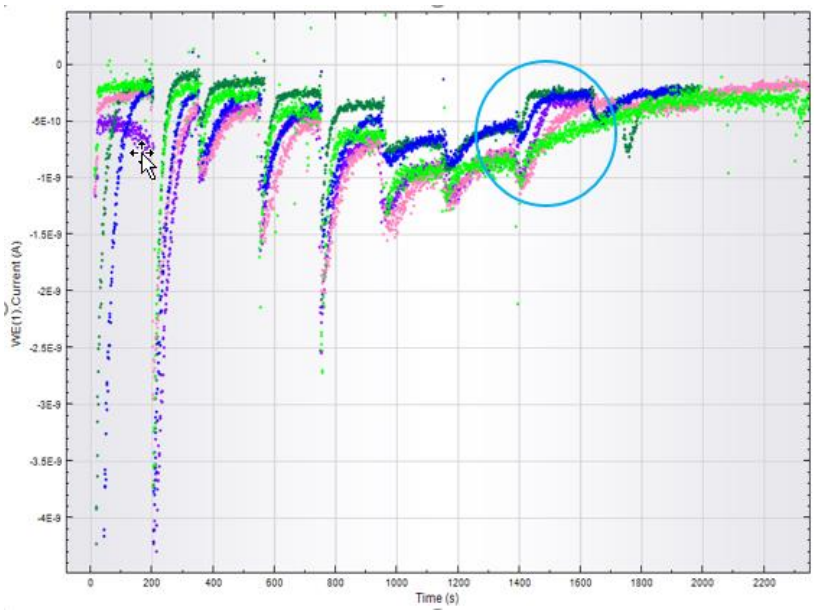

Figure 29. Second experimental series varying CDH concentration in correlation to LPMO. The color code is explained in Table 4.

Comparing both experimental series, a clear trend was visible. With decreasing the amount of CDH, slopes were notably flatter, and the reaction time required to deplete the peroxide increased.

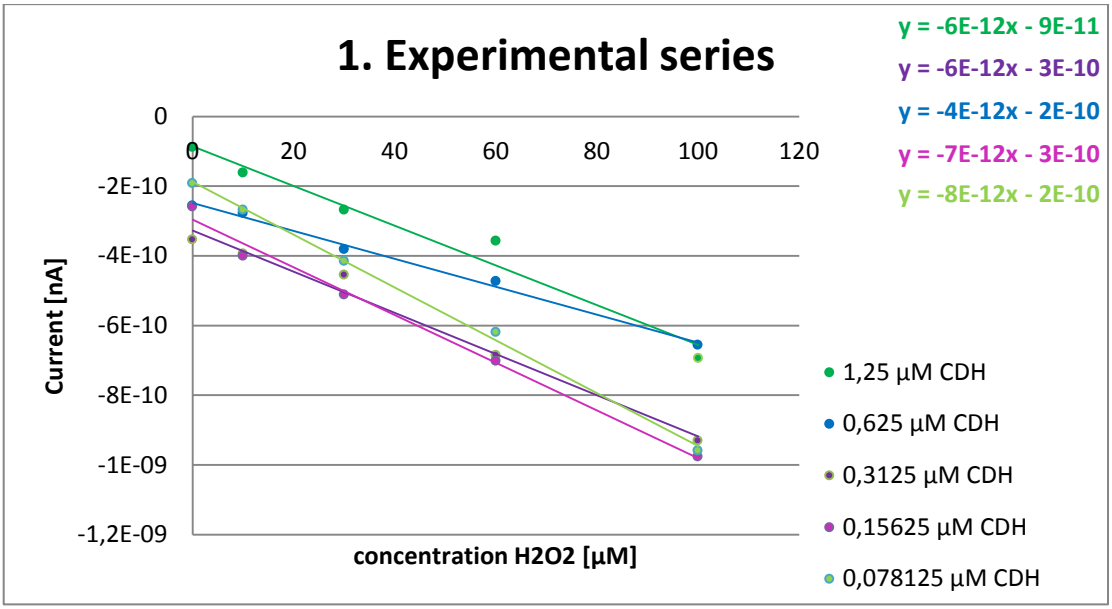

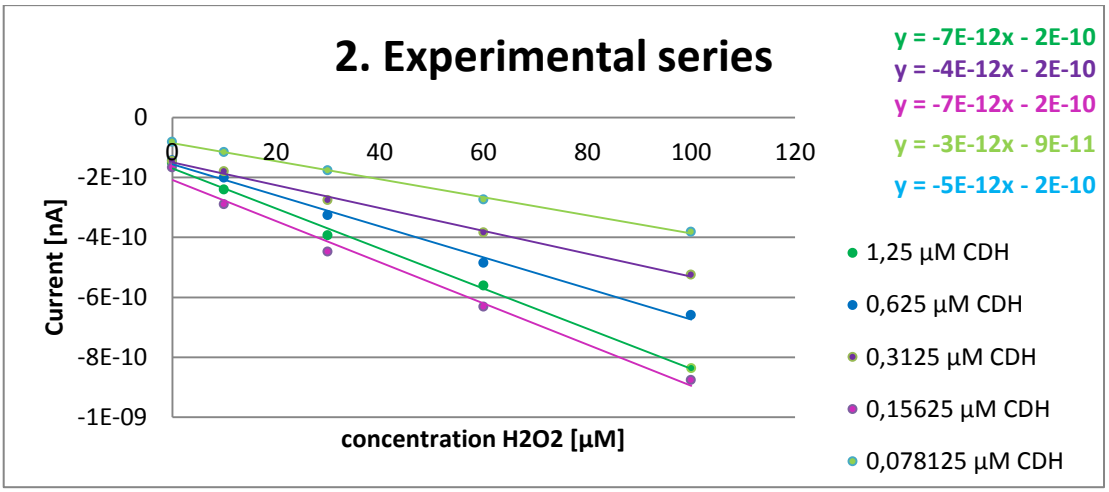

Figure 30. H_2O_2 calibration. experiments: varying ratios LPMO to CDH.

- Calculation of rates:

1. Use linear part of the reaction slope
2. Calculate slope [A/min]
3. Note calibration slope
4. Calculate enzyme factor

$$enzyme\ factor = \frac{volume\ in\ the\ cell}{volume\ LPMO\ in\ the\ cell * slope\ calibration}$$

5. Rate in [U/mL]

$$rate = calibration\ slope * enzyme\ factor$$

6. Calculate concentration of LPMO [g/L]

$$concentration\ \left[\frac{\mu mol}{L}\right] * M\ LPMO\ \left[\frac{\mu g}{\mu mol}\right] = 1.25 * 34282 = 42852.5\ \left[\frac{\mu mol}{L}\right] = 0{,}0429\ \frac{g}{L}$$

7. Calculate specific activity in [U/mg]

8. Calculate Rate in [s^{-1}]

Table 5. Calculation of rates varying ratios LPMO to CDH from 1, 2, 4, 8 and 16 (Three experimental series were performed).

1. reaction series								
ratio	**Slope [A/min]**	**calibration slope [A/µM]**	**volume in cell [µL]**	**volume enzyme in cell [µL]**	**enzyme factor [µM/A]**	**[U/mL]**	**[U/mg]**	**rate [s-1]**
1	6.9E-10	6.0E-12	5221.41	7.88	1.1E+14	76	1779	1016
2	4.0E-10	4.0E-12	5211.15	7.88	1.7E+14	66	1547	884
4	4.8E-10	6.0E-12	5206.01	7.88	1.1E+14	52	1221	698
8	3.1E-10	7.0E-12	5203.45	7.88	9.4E+13	29	672	384
16	4.1E-11	8.0E-12	5213.68	7.88	8.3E+13	3	79	45
2. reaction series								
1	1.1E-09	7.0E-12	5221.41	7.88	9.5E+13	106	2482	1418
2	5.5E-10	5.0E-12	5211.15	7.88	1.3E+14	73	1695	969
4	2.4E-10	4.0E-12	5206.01	7.88	1.7E+14	39	919	525
8	4.3E-10	7.0E-12	5203.45	7.88	9.4E+13	41	946	541
16	1.9E-12	3.0E-12	5213.68	7.88	2.2E+14	0	10	5
3. reaction series								
1	1.2E-09	9.0E-12	5221.41	7.88	7.4E+13	88	2062	1178
2	2.4E-09	3.0E-11	5211.15	7.88	2.2E+13	53	1235	705
8	3.0E-10	8.0E-11	5203.45	7.88	8.3E+12	2	58	33

With varying the ratio LPMO to CDH over 1, 2, 4, 8 and 16 rates of LPMO decreased. Despite a high standard deviation, a clear trend was visible as shown in Table 6

Table 6. Reaction rates for peroxide consumption for different CDH concentrations.

ratio	average [s-1]	standard deviation
1	1204	202.1
2	853	134.3
4	611	121.8
8	319	259.9
16	25	28.4

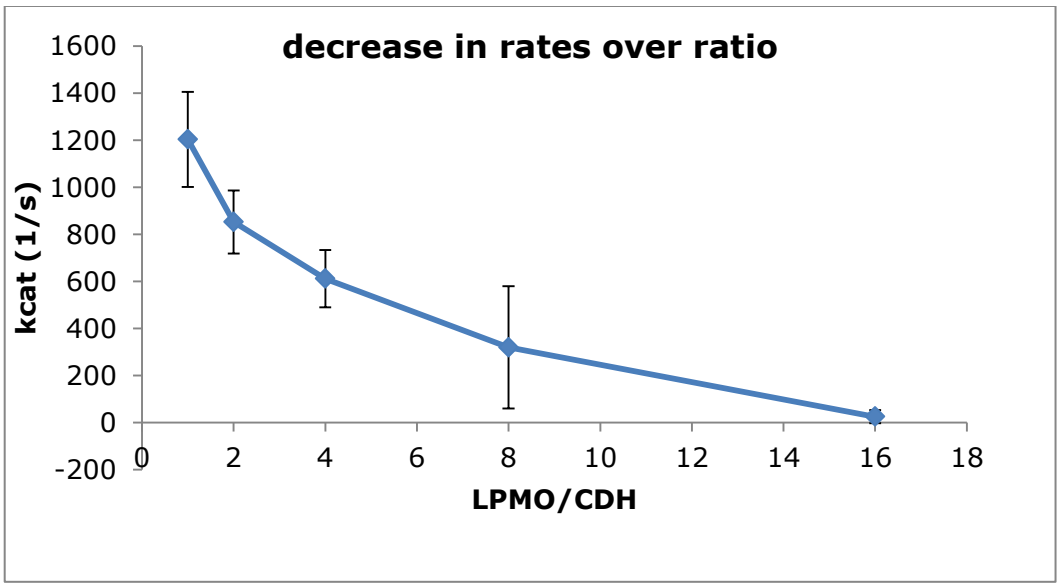

Figure 31. Decrease in rates over decreasing ratios LMPO to CDH.

2.3.2 Product analysis

Products were analyzed using HPAEC. To be able to characterize and quantify all peaks, standards with known concentrations were run as reference.

2.3.2.1 Checking purity of the enzymes

To check whether there are any cellulase impurities in the enzymes LPMO9C, *Mt*CDH IIA, *Mt*DH IIA, *Mt*CDH $Oxy^{+}$and *Mt*DH Oxy^{+} conversion tests with oligosaccharide substrateswere performed. To all CDH variants, 0.025 g/L cellohexaose was added and incubated over night at 30 °C. To stop the

reactions, 200 mM sodium hydroxide (ratio 1:1) was added. After centrifugation at 15,000 rpm for 5 min, samples were analyzed for reaction products using HPAEC. The expected outcome of an oxidation reaction by the CDHs in absence of endoglucanases is cellohexaonic acid. This experiment resulted in gluconic acid, cellobionic acid and cellotrionic acid, which indicates that all four CDH preparations were contaminated and contained an unspecific endoglucanase. This can be seen in Figure 32.

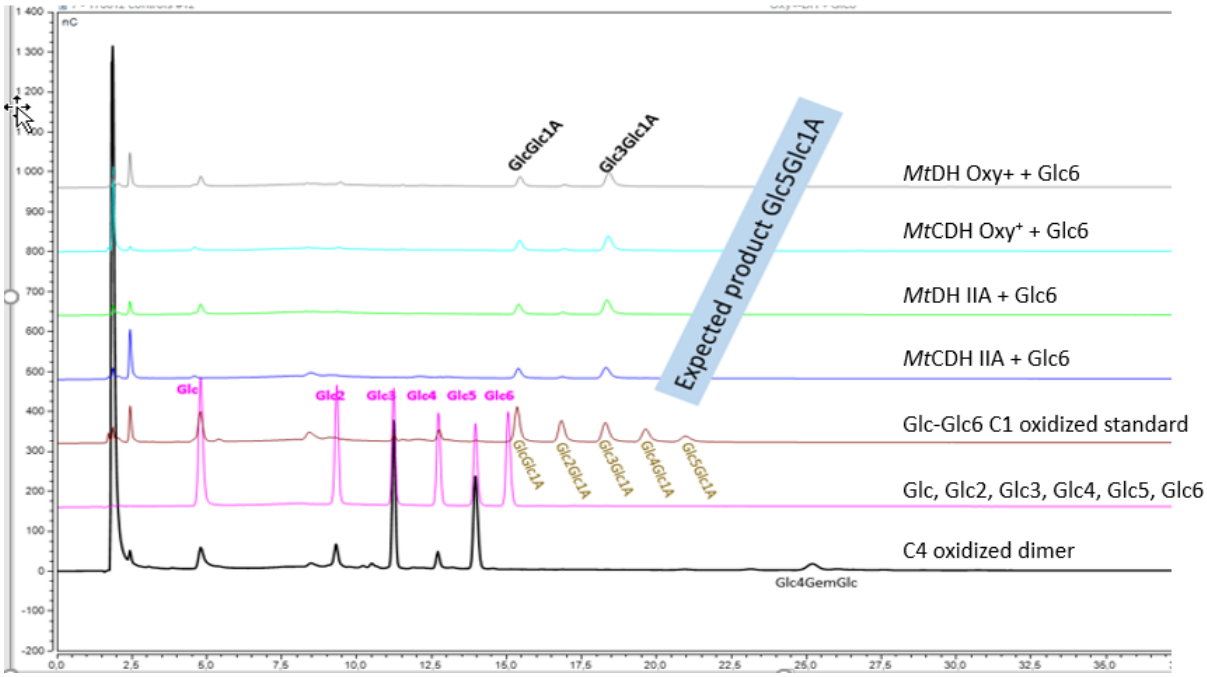

Figure 32. Purity of CDH variants. The purity of the LPMO was checked in several reactions. The composition can be seen in Table 7. Reaction 2. and 4. did not contain any electron donor in the form of ascorbic acid, which should render the enzyme inactive and no products should be detected. In reaction 1. and 3., LPMO should oxidize cellohexaose to the corresponding ketoaldose/gemdiol.

Table 7. purity check NcLPMO: compostion of reactions.

1. reaction	X	0.025 g/L cellohexaose	1 µM LPMO	50 mM buffer	1 mM ascorbic acid
2. reaction	X	0.025 g/L cellohexaose	1 µM LPMO	50 mM buffer	X
3. reaction	0.2 % PASC		1 µM LPMO	50 mM buffer	1 mM ascorbic acid
4. reaction	0.2 % PASC		1 µM LPMO	50 mM buffer	X

In all four control reactions cellohexaose was completely degraded. In the reactions without ascorbic acid, LPMO was inactive, because no C4 oxidized products were visible, even though cellohexaose was degraded. When ascorbic acid was present, C4 oxidized dimers and trimers as well as some double oxidized products were found. These results show that there was an endoglucanase contamination in the LPMO.

2.3.2.2 Determination of the optimal reaction time and lactose concentration

As seen in Figure 33, CDH oxidizes products released from cellulose by cellulases and LPMOs.

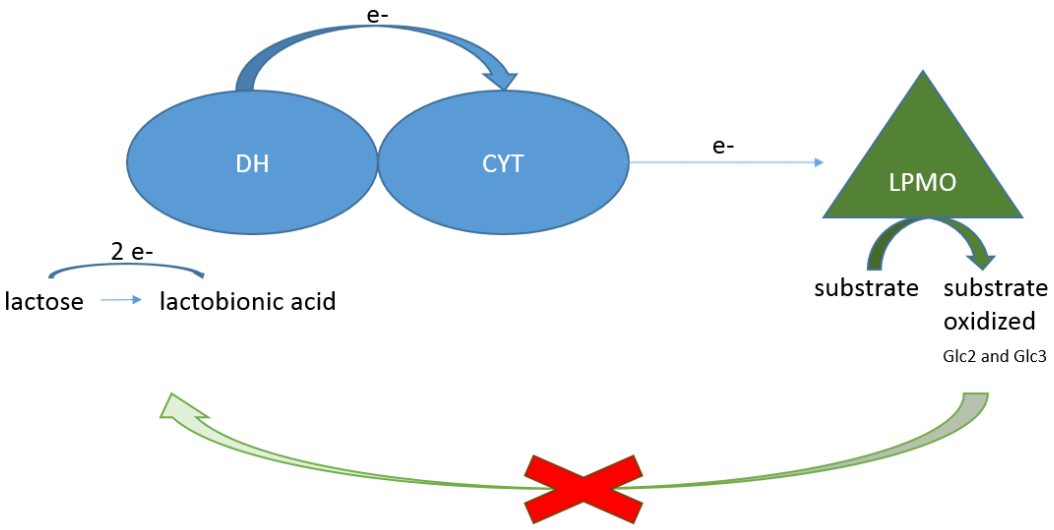

Figure 33. Interaction between CDH and LPMO. electron transfer and product interaction.

To avoid this effect, lactose was added as an alternative substrate for CDH. This was done in order to be able to distinguish and quantify LPMO products in follow up reactions from CDH reactions products. By adding a surplus of lactose, CDH should preferentially oxidize lactose instead of the LPMO products, which are only present in low amounts. To determine which concentration of lactose is necessary to obtain this effect, the concentration of lactose was varied from 1, 5, 10 to 15 mM. To simulate LPMO products, cellobiose and cellotriose were added in two concentrations: 0.01 g/L to simulate the early phase reaction products, and 0.025 g/L as late phase products.

Furthermore, it was a point of interest when this effect stops and CDH uses LPMO products again. To find out the optimal reaction time the reactions were stopped after 30, 60, 120, 360 and 1440 min.

First the experiments were performed using only *Mt*CDH IIA. Based on these results, the variants were tested for 1 mM and 15 mM lactose concentration and samples were taken after 3h, 6h and 22 h of incubation.

The evaluation was based on the peak area and not on the concentration, which means it was not a quantitative analysis, but allowed for an analysis of a trend.

CDH oxidizes lactose to lactobionic acid. Either low or high concentrations of cellobiose and cellotriose, as well as low or high concentration of lactose led to similar results. (Figure 34)

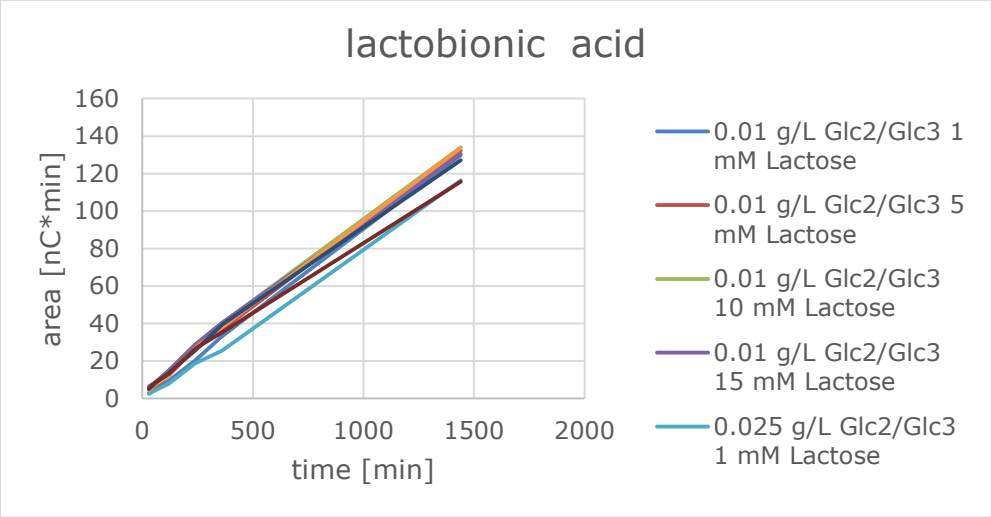

Figure 34. lactobionic acid production *Mt*CDH IIA. initial lactose concentration 1, 5, 10, 15 mM.

Cellobionic acid as well as cellotrionic acid are products of cellobiose and cellotriose oxidation. When the lactose concentration was kept at 15 mM, hardly any potential oligosaccharides released by LPMO were oxidized. With lower concentrations, more cellobionic acid and cellotrionic acid were produced. At a low concentration of LPMO products, almost no oxidation by CDH occurred (high ratio between lactose and cello-oligosaccharides). (Figure 35) As a consequence, follow up reactions with *Mt*CDH IIA and *Nc*LPMO were incubated for a maximum of 6 h to be able to distinguish and quantify LPMO products.

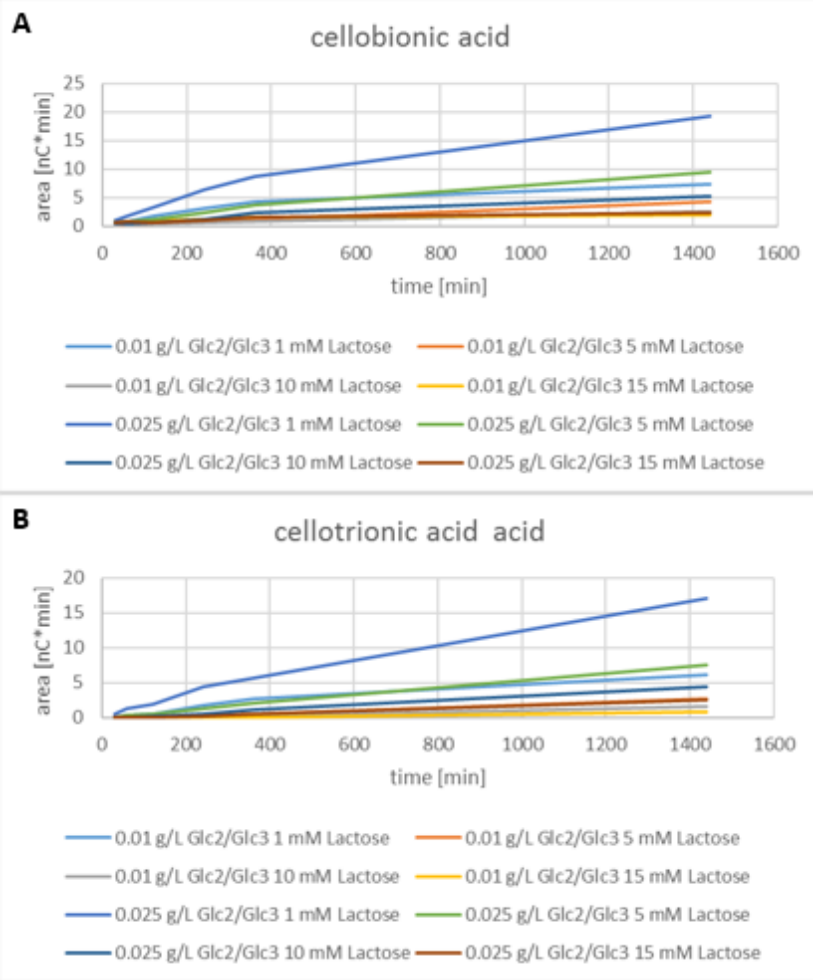

Figure 35. *Mt*CDH IIA supported cellobionic and cellotrionic acid production. A: cellobionic acid production out of cellobiose. B: cellotrionic acid production out of cellotriose.

In a control reaction, cellobiose oxidation by CDH was quantified and compared to the formation of cellobionic acid. Expectedly, more cellobiose was consumed at lower lactose concentrations.

In view of the results obtained with *Mt*CDH IIA, a high concentration of 15 mM lactose and a low concentration of 1 mM lactose led to low and comparable amounts of lactobionic acid. *Mt*DHIIA is a variant containing only the dehydrogenase domain of full-length CDH, which was denoted "DH" in Figure 35. All other abbreviations are explained in Table 8.

Table 8. Enzyme abbreviations used in the figures.

name	Abbreviation in the following graphs
*Mt*CDH IIA	WT
*Mt*DH IIA	DH
*Mt*CDH Oxy^+	Oxy
*Mt*DH Oxy^+	OxyDH
1 or 15	Lactose concentration [Mm]

*Mt*DH IIA led to lactobionic acid signals between 200 and 300 nC*min after 24 h. For *Mt*CDH IIA and *Mt*DH IIA, a linear increase in peak area was visible. At a concentration of 1 mM lactose comparable amounts of lactose were consumed by *Mt*CDH Oxy^+ and *Mt*DH Oxy^+ after three h of incubation. As samples contained 15 Mm lactose, lower amounts of cellobionic acid were produced. This is shown in Figure 36.

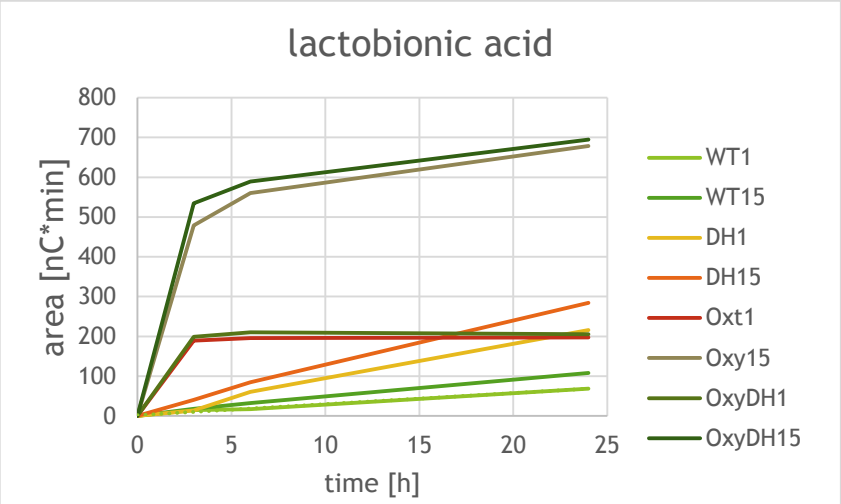

Figure 36. Lactobionic acid production CDH variants. 1 and 15 mM lactose concentration.

Cellobionic acid was considered as an LPMO product oxidized by CDH. When the lactose concentration was kept at 15 mM, *Mt*CDH IIA and *Mt*DH IIA preferred lactose as a substrate over cellobiose, whereas *Mt*CDH Oxy$^+$ and *Mt*DH Oxy$^+$ already produced high amounts of cellobionic acid after 3 h of incubation. At the lower lactose concentration of 1 mM, all variants produced high amounts cellobionic acid within 3 h. (Figure 37) It can be concluded that under these conditions lactose did not prevent LPMO products from degradation anymore, which makes quantification of *Nc*LPMO9C products difficult.

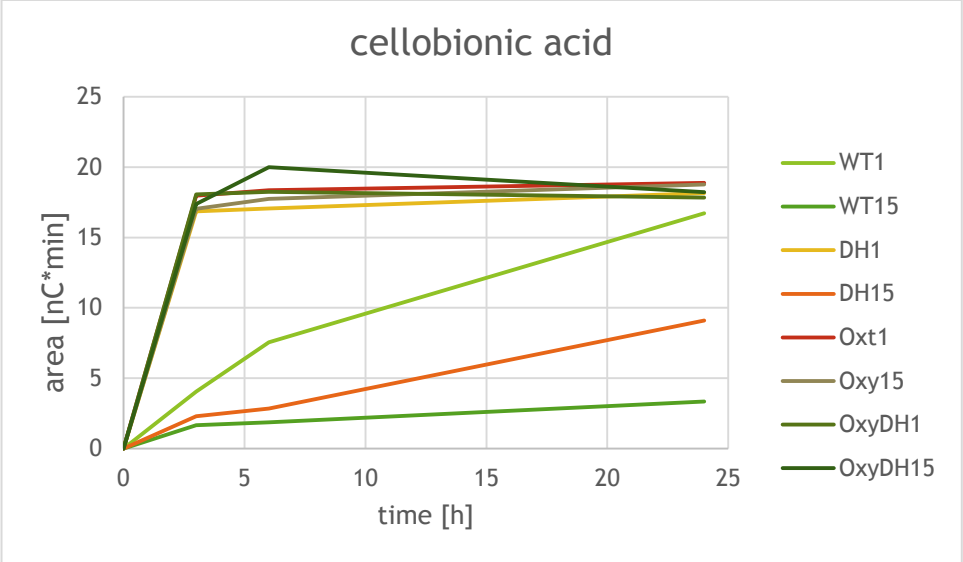

Figure 37. Cellobionic acid production CDH variants. 1 and 15 mM lactose concentration.

As a control experiment cellobiose conversion by CDH was followed. (Figure 38) Cellobiose was oxidized very fast and in high amounts. At high concentrations of lactose, the effect of preferring lactose as a substrate could be proved for *Mt*CDH IIA and *Mt*DH IIA. With the lower lactose concentration (1 mM), cellobiose was consumed faster and more efficient. This fits to the results observed for the generation of cellobionic acid. *Mt*CDH Oxy$^+$ and *Mt*DH Oxy$^+$ consumed cellobiose completely within few h and lactose had no preventing effect anymore.

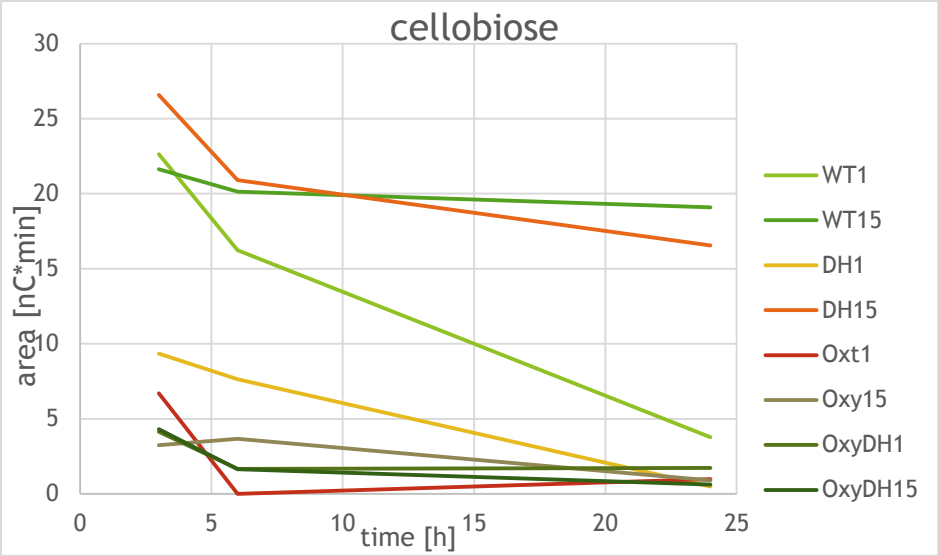

Figure 38. Cellobiose consumption CDH variants. 1 and 15 mM lactose concentration.

2.3.2.3 Validation of electrochemical data

The hypothesis that addition of H_2O_2 to LPMO increases the amounts of products was tested in the following experiments shown in Figures 39 and 40. According to previous studies (33), it is known that adding high amounts of H_2O_2 at once (>100 µM) leads to inactivation of LPMO. To avoid loss of enzyme activity, H_2O_2 was added in two sequential steps. This experiment was performed with electrochemistry and validated using HPLC.

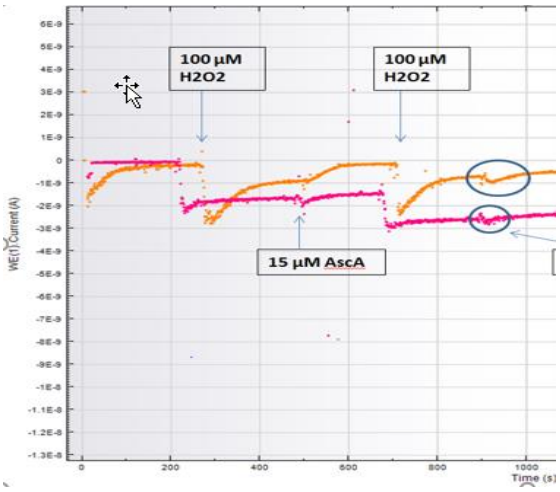

Figure 39. Adding two times 100 µM H_2O_2 and 15 µM ascorbic acid leads to H_2O_2consumption by the LPMO. (orange) method used: electrochemistry.

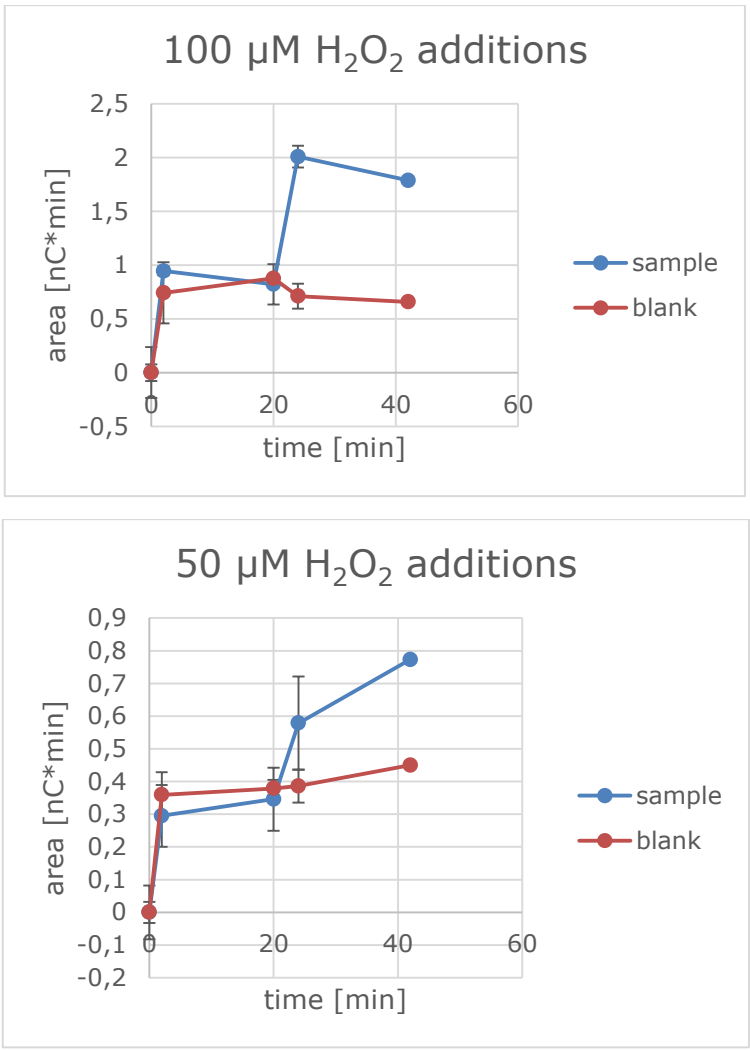

Figure 40. Adding two times 100 µM H_2O_2 and 15 µM ascorbic acid leads to twice as much products. Samples were analyzed by HPAEC.

The reaction contained 6.6 mg/mL PASC, 100 µM H_2O_2 and 1.25 µM LPMO. After 2 and 20 min, samples were taken and analyzed for LPMO reaction productsby HPAEC. After 22 min, 100 µM H_2O_2 and 15 µM ascorbic acid were added to the reaction, and at 24 and 42 min samples were taken. The whole procedure was repeated by adding 50 µM H_2O_2 twice. A blank run was treated as the sample except that H_2O_2 and ascorbic acid were added once. Products of these samples were checked using HPLC.

After two min, low amounts of products were already detectable. The amounts of products remained at the same level after 20 min of incubation. Adding H_2O_2 and ascorbic acid led to an increase in products by a factor of two.

2.3.2.4 H_2O_2 production of CDH variants

As H_2O_2 is thought to be a substrate of LPMO, it was of major interest to investigate the rate of oxygen reduction of each CDH variant, to be able to relate these data to the LPMO kinetics. The Amplex Red/horseradish peroxidase assay according to Kittl et al (34) was used to measure H_2O_2. Concentrations are shown in Table 9.

Table 9. Amplex Red assay. Assay stock solutions and concentrations in the reaction.

Solutions for Amplex Red Assay	Concentration In reaction setup
Amplex Red	100 µM
*Mt*CDH IIA	1 µM
*Mt*DH IIA	0.5 µM
*Mt*CDH Oxy^+	0.025 µM
*Mt*DH Oxy^+	0.010 µM
lactose	15 mM
Horse radish peroxidase	5 U/mL
H_2O_2 standards	5 µM
	10 µM
	15 µM
	20 µM

Standards, samples and blanks were prepared in a 96-well plate with a final volume of 50 µL in each well. A so called "mastermix", containing phosphate buffer, horse radish peroxidase and Amplex Red in DMSO, was prepared. Forty µL "mastermix" were added to each well. To start the reaction, 10 µL of lactose were added as substrate for CDH immediately before starting the measurement, resulting in a final lactose concentration of 15 mM. This assay is based on an accessible oxygen-reducing side-reaction of LPMO. CDH oxidizes lactose to lactobionic acid and produces H_2O_2, which is reduced to oxygen by horse radish peroxidase. The peroxidase converts Amplex Red to Resorufin in a coupled reaction which is visible at 540 nm. (34) Results are shown in Table 10.

Table 10. H_2O_2 production CDH variants.

	Rate [µmol/min]	Standard deviation	Ratio compared to *Mt*CDH IIA
*Mt*CDH IIA	0.370	0.17	1
*Mt*DH IIA	1.148	0.34	3.1
*Mt*CDH Oxy^+	55.28	55.28	149
*Mt*DH Oxy^+	118.44		320

If the CDH lacks the cytochrome domain, approximately twice as much H_2O_2 was produced when compared to the full-length enzyme. *Mt*DH Oxy^+ is 149 times more efficient in providing H_2O_2 to LPMO. According to these results, it was assumed that about 150 times less *Mt*CDH Oxy^+ is necessary to reduce the same amount of *Nc*LPMO compared to the wild type *MtCDH IIA*.

2.3.2.5 Testing different ratios CDH to LPMO

As described above, it was not possible to quantify the products of the C4 oxidizer *Nc*LPMO9C because CDH consumes also cellobiose and cellotriose. It was decided to use another LPMO, which is a C1 oxidizer. In the following, the bacterial, family AA10 LPMO "CBP21", which is active on chitin, was used instead. Its main product, chitobionic acid, is not consumed by CDH.

To test the interaction between CBP21 and CDH, and validate the electrochemical experiments, different ratios of CDH to CBP21 were incubated and products analyzed. The concentration of CBP21 was kept at 1 µM while the concentration of CDH was varied from 3, 1.5, 1, 0.500, 0.250, 0.125, 0.0313, 0.0156 and 0.0078 µM.

Both, the full lengths CDHs *Mt*CDH IIA and *Mt*CDH Oxy^+, were tested in combination with the LPMO. Ten g/L β-chitin as substrate for CBP21 and 15 mM lactose as substrate for the CDHs were added. Incubation was performed for 1h and 24h at 40 °C under constant agitation (1000 rpm). Sixty µL of the samples were taken and filtrated using a 96-well filter plate. The samples were boiled for ten min to inactivate and precipitate the enzymes. Thirty-five µL sample were

prepared in an Eppendorf tube and 35 µL chitobiase was added to degrade all oxidized products to N-acetylglucosamin and chitobionic acid. Chitobionic acid was visible and quantifiable at the HPAEC.

After one hour of incubation a ratio three to one for the *Mt*CDH IIA to CBP21 led to the highest amounts of chitobionic acid. For the varient *Mt*CDH Oxy^{+} products were even higher when using only 62.5 nM of CDH. The amount of chitobionic acid produced at each ratio can be seen in Figure 41.

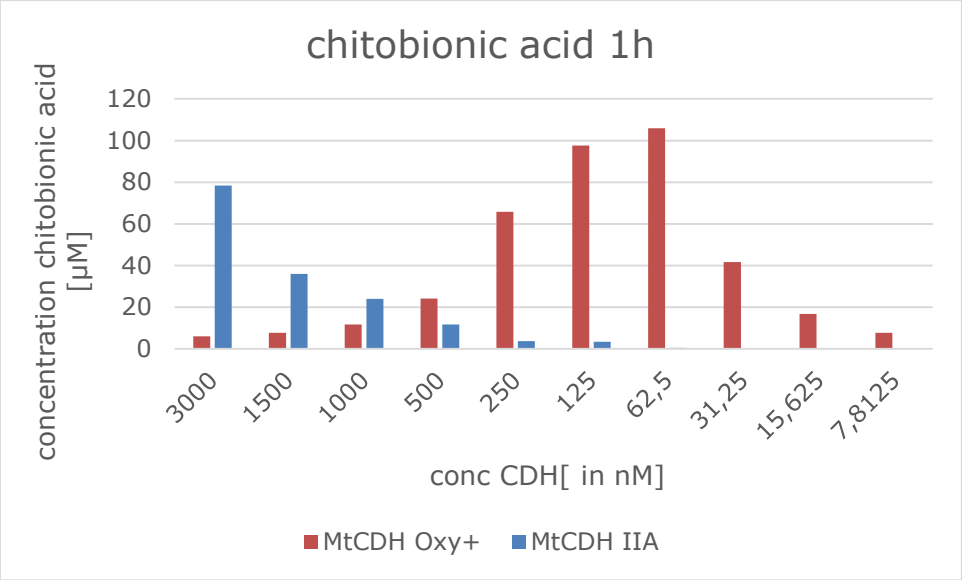

Figure 41. Chitobionic acid production after 1 h. Testing different ratios CDH to LPMO. In blue:WT. and in orange: Oxy+mutant.

After 24 h of incubation, *Mt*CDH IIA in combination with CBP21 produced the highest amounts of oxidized products with a CDH concentration of 1.5 µM. When using *Mt*CDH Oxy^{+} the amount of necessary CDH to reduce the LPMO could be reduced by a factor of 48, while still similar amounts of oxidized chitooligosaccharides were generated.

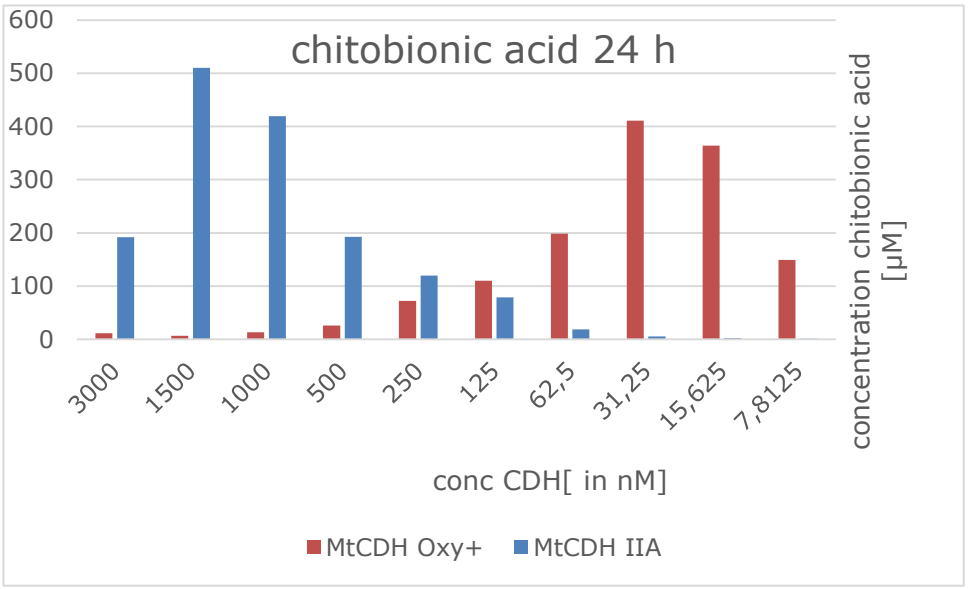

Figure 42. Chitobionic acid production after 24 h. Testing different ratios CDH to LPMO. In blue:WT. and in orange: Oxy+mutant.

When using *Mt*CDH Oxy$^+$, the amounts of chitiobionic acid after one hour and 24 h were approximately the same for the ratios 1:3 to 1:125. It can be assumed that CBP21 was deactivated by a too high H_2O_2 concentration produced by *Mt*CDH Oxy$^+$. The shift from the optimum ratio after one hour from 62.5 nM to 31.25 nm *Mt*CDH Oxy$^+$ after 24 h as well as the shift from 3 µM to 1.5 µM *Mt*CDH IIA can be also explained by a slow deactivation of LPMO by H_2O_2. (Figure 43)

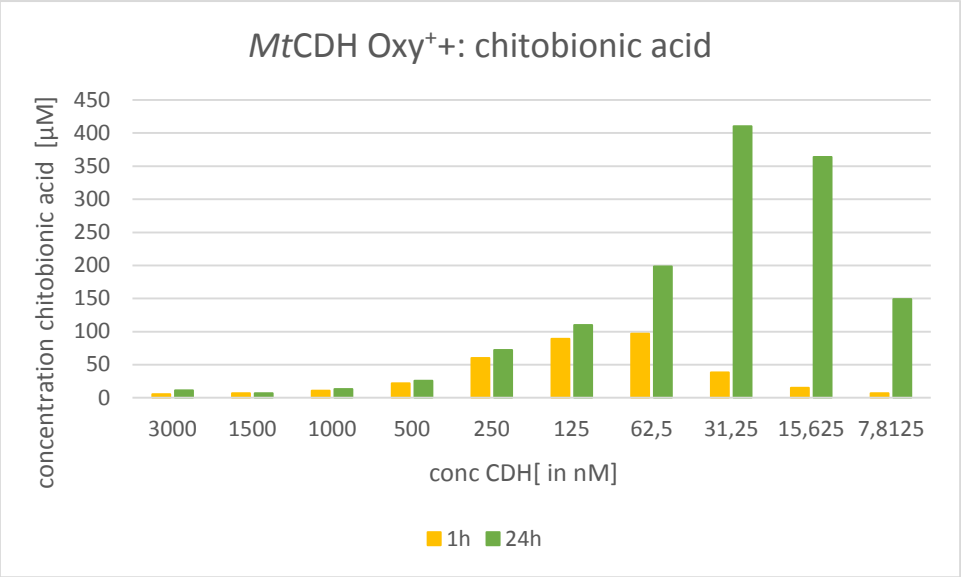

Figure 43. *Mt*CDH Oxy$^+$ + chtiobionic acid production after 1 and 24 h. testing different ratios of CDH to LPMO.

2.3.2.6 Time course MtCDH IIA and MtCDH Oxy$^+$

Time-dependent reactions were made with two CDH variants (full-length *Mt*CDH IIA and *Mt*CDH Oxy$^+$) together with CBP21 using the CDH concentrations that gave the most stable kinetics in previous experiments. For *Mt*CDH IIA, a concentration of 1500 nM was used whereas for the *Mt*CDH Oxy$^+$ 31.25 nM were used. Samples were taken after 15, 30, 45, 60, 90, 180 and 1440 min.

As is shown in Figure 44, linear kinetics were obtained for both CDH variants. Based on the linear increase in chitobionic acid production for 180 min, the catalytic rate of LPMO using *Mt*CDH IIA as an electron supplier lead a catalytic activity of 0.74 µmol/min, and *Mt*CDH Oxy$^+$ showed a catalytic activity of 0.95 µmol/min.

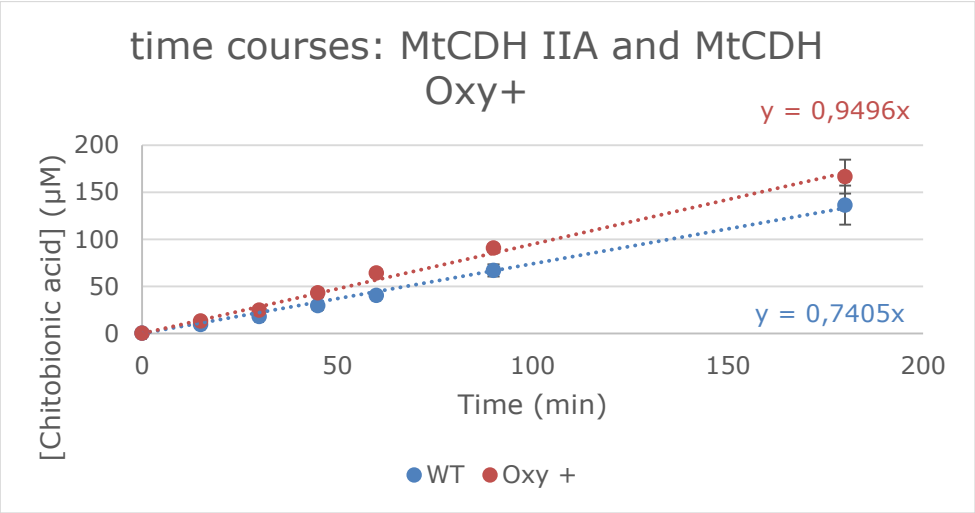

Figure 44. Time course MtCDH IIA and MtCDH Oxy+ in interaction with CBP21.

2.3.2.7 Testing MtDH IIA and MtDH Oxy$^+$ with and without ascorbic acid

As known from previous experiments, the DH domains produce approximately twice as much H_2O_2 as the full-length CDHs. In view of their higher H_2O_2 production, half the concentration of the full length CDHs should lead to the same reaction kinetics of CBP21 observed for the CDH holoenzymes. Three concentrations of the wild-type DH domain were tested (1500, 1000 and 500 nM), while for the Oxy$^+$ the concentrations were lowered by a factor of approximately 50 (31.25; 15.625 and 7.8125 nM). One set of these concentrations were incubated with a low concentration of ascorbic acid (i.e. 100 µM ascorbic acid) and one set was incubated without reducing agent as control experiment. Fifteen mM lactose was added as a substrate for the CDHs and 20 mM Bis Tris, pH 6.0, was used as buffer. Ten g/L β-chitin was used as a substrate for 1 µM CBP21. One control reaction was performed using only ascorbic acid (100 µM) without CDH.

With an increase in the *Mt*CDH Oxy$^+$ concentration from 7.8125 to 31.25 nM in the reactions containing ascorbic acid, the concentration of chitobionic acid, the product of CBP21, increased linearly. Without adding any reductant to the reactions, no product formation was expected to occur in consideration of the current state of research, which shows that the cytochrome *b*-containing domain of CDH is essential for the reduction of the LPMO active site.(20) Contrary to these results, in the presented reactions high amounts of chitobionic acid were

produced in a DH -dependent reaction. This effect was also visible for the wild-type-DH domain, without adding a reductant in Figure 45.

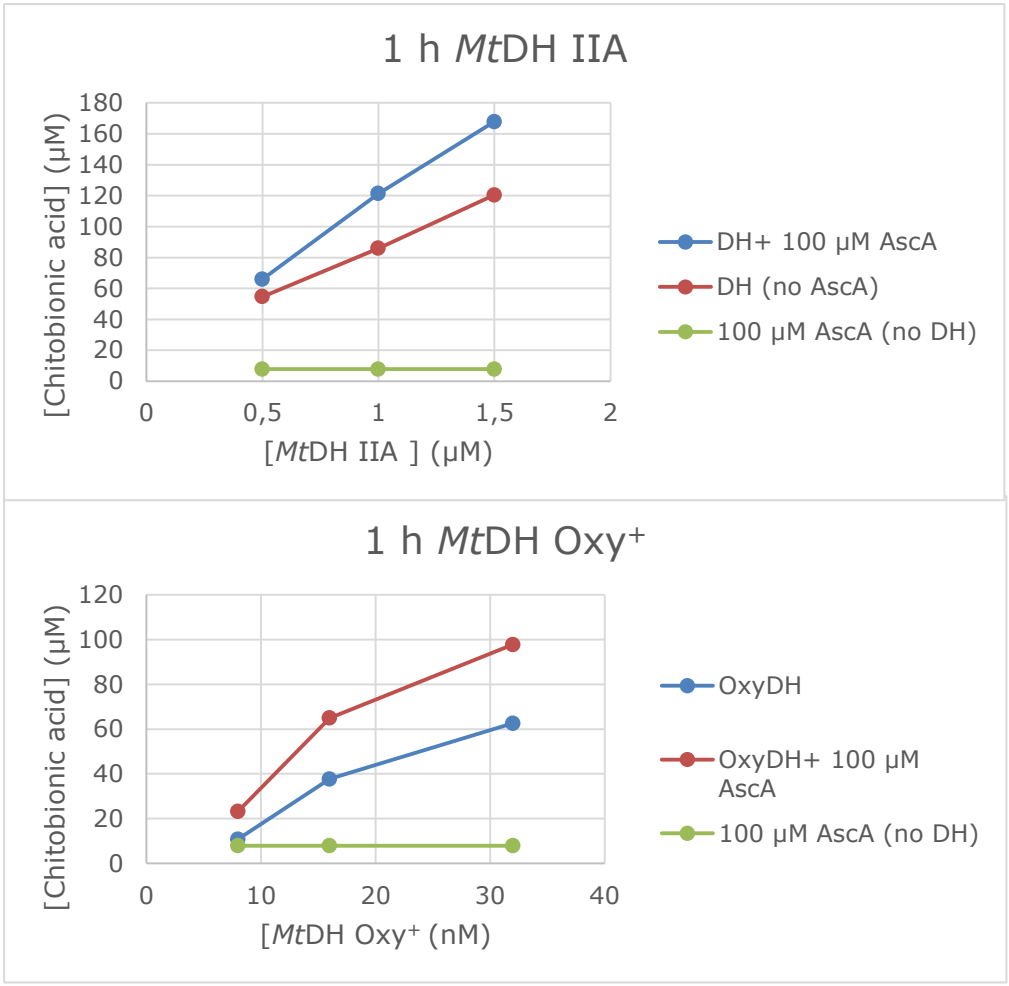

Figure 45. Short domain CDHs in interaction with CBP21 and the influence of adding ascorbic acid after 1 h incubation; Ascorbic acid is not necessary to activate LPMO.

After 9 h of incubation, shown in Figure 46, the product formation of the wild-type DH stopped. It is likely that either of the enzymes (CDH or LPMO), or both, were inactivated, or that the substrate was saturated, since reactions leveled off at a product concentration of approximately 300 µM. Deactivation may have also occurred as a result of an overproduction of H_2O_2 produced by the CDH variants.

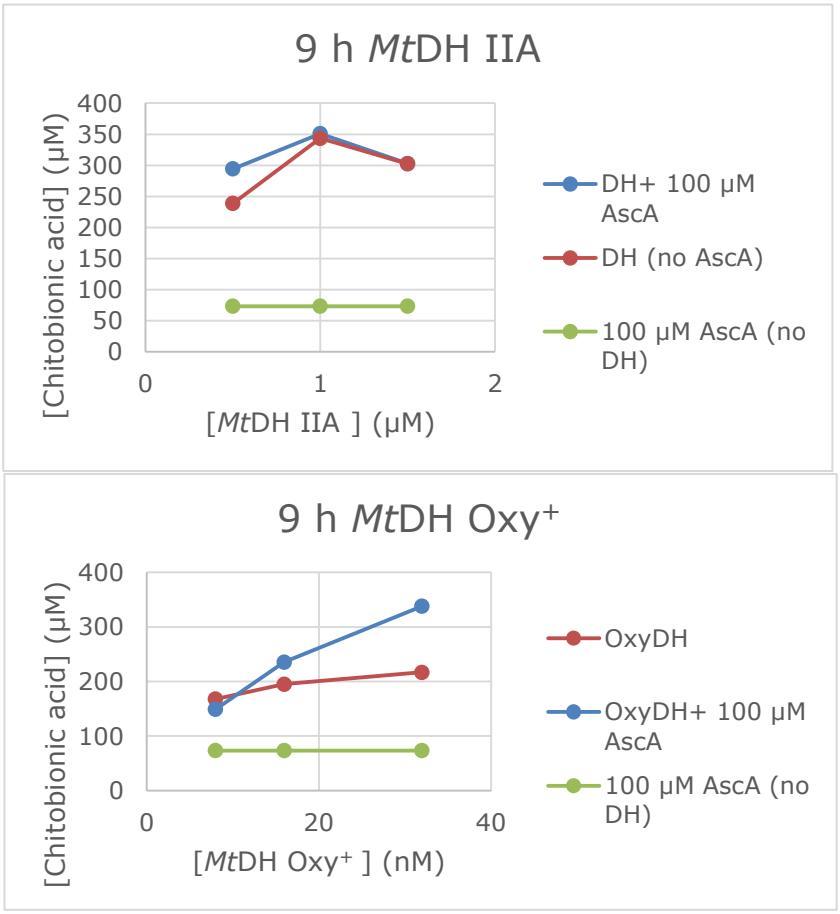

Figure 46. Short domain CDHs in interaction with CBP21 and the influence of adding ascorbic acid after 9 h incubation; ascorbic acid is not necessary to activate LPMO.

2.3.2.8 Activation of DH domain without ascorbic acid

Regarding the results mentioned before, it seems likely that addition of reluctant is not necessary to reduce LPMO. Several hypotheses regarding a possible reaction mechanism were tested in the following.

Superoxide hypothesis

The DH domain of the CDH produces H_2O_2 via reduction of molecular oxygen. Superoxide, which can be formed by the cytochrome domain of CDH, has been shown to reduce LPMO(33). To test this hypothesis, superoxide dismutase (SOD) was added to convert superoxide into H_2O_2. In presence of a higher amount of H_2O_2, higher product formation should be observed, whereas removal of superoxide should inhibit the LPMO reaction as it cannot become reduced anymore.

First, the amount of H_2O_2 being produced by the CDH variants in combination with 1, 10 and 100 nM SOD was tested. (Figure 47) The addition of 1 nM SOD lead to no significant increase in H_2O_2 production, but adding 10 or 100 nM SOD increased the peroxide formation rate. As a first test, this experiment was done with the *Mt*DH IIA domain.

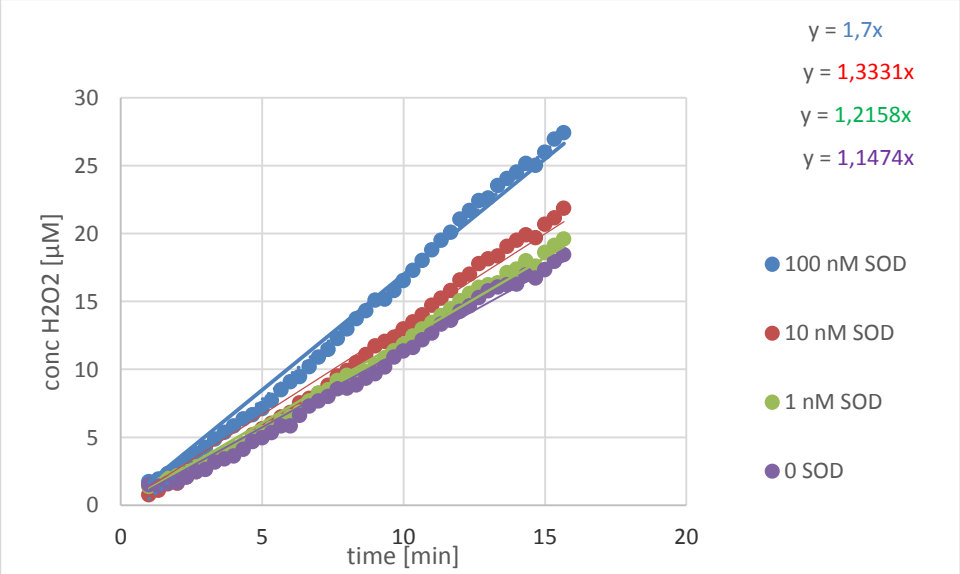

Figure 47. impact on H_2O_2 formation by adding 1,10 and 100 nM SOD to *Mt*DH IIA.

To validate these results, all 4 CDH variants were tested by adding 10 nM and 100 nM SOD. (Figure 48)

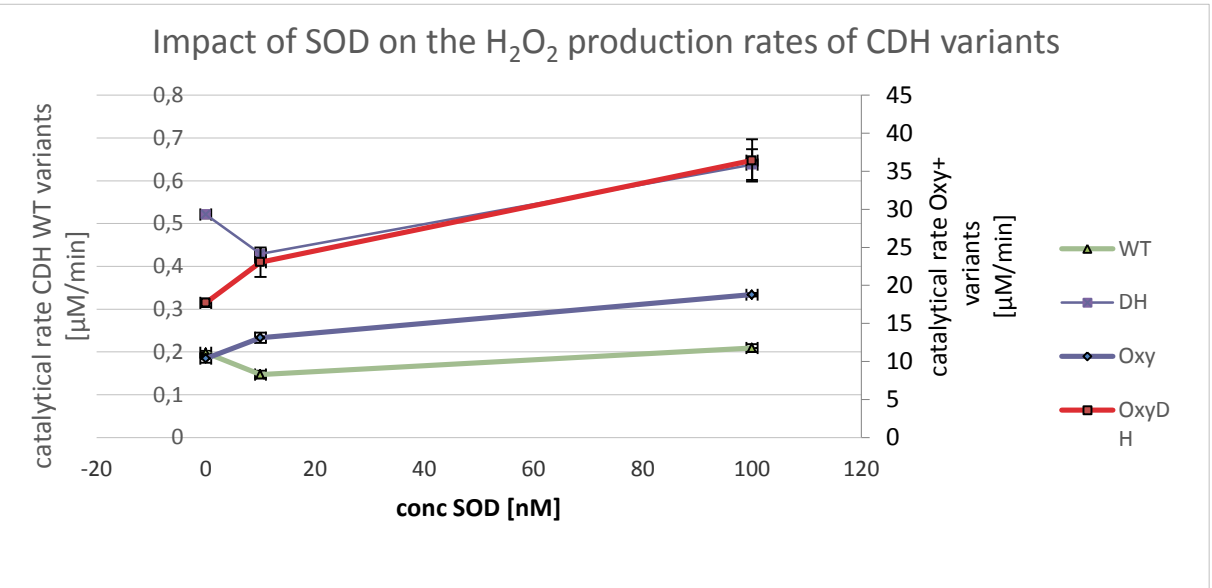

Figure 48.Impact of SOD on H_2O_2 production rates of CDH variants.

To summarize these results, the peroxide production of all CDH variants could be improved by addition of SOD. For the full-length *Mt*CDH IIA this effect was not observed. The cytochrome domain could protect the DH domain and hamper superoxide production. H_2O_2production of the DH domains was twice as much higher as for the full lengths CDHs. Probably this is because electrons do not have to be transferred to the cytochrome.

Next, the influence of superoxide formed by CDH was tested on product formation by LPMO.

A concentration of 31.25 nM *Mt*DH Oxy^{+} was added to a reaction containing 1 µM CBP21, 10 g/L β-chitin as substrate for the CBP21 and 15 mM lactose as a substrate for CDH. The reaction was carried out in 50 mM BIs-Tris buffer, pH 6.0. Samples were taken after 15, 30, 45, 60, 90, 120 min and 22 h. No ascorbic acid was added. In another experimental setup, 1.5 µM *Mt*DH IIA were used instead of the *Mt*DH Oxy^{+} . All other conditions were the same. In another experimental series, the same experiments as above were performed in presence of 10 nM or 100 nM SOD. Chitobionic acid amounts can be seen in the figure 49. In 49 A LPMO was activated by *Mt*DH Oxy^{+} whereas in 49 B *Mt*DH IIA was used.

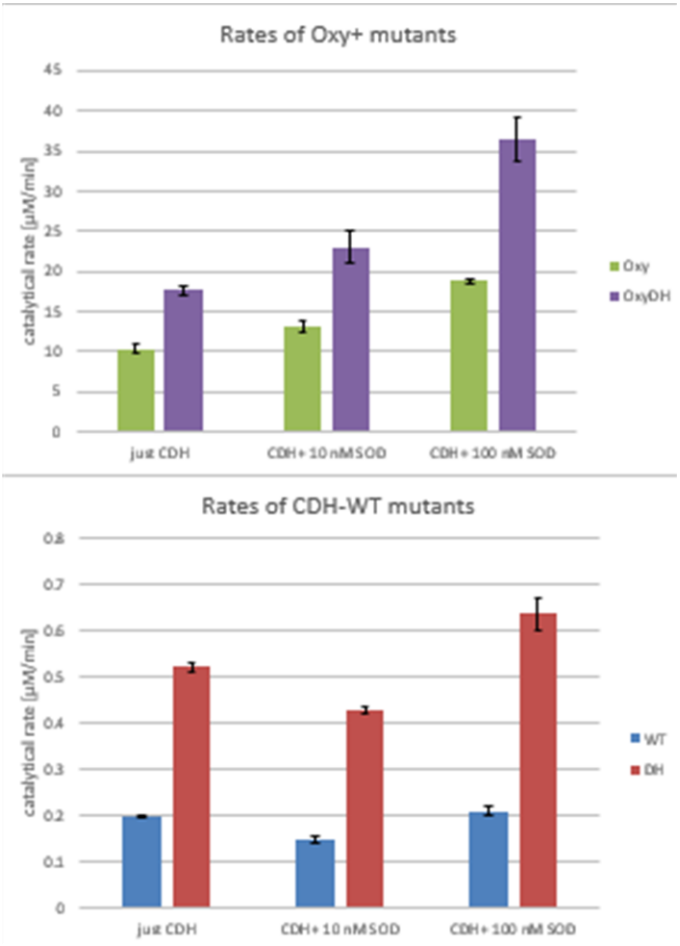

Figure 49. H_2O_2 production rates; addition of 10 and 100 nM SOD.

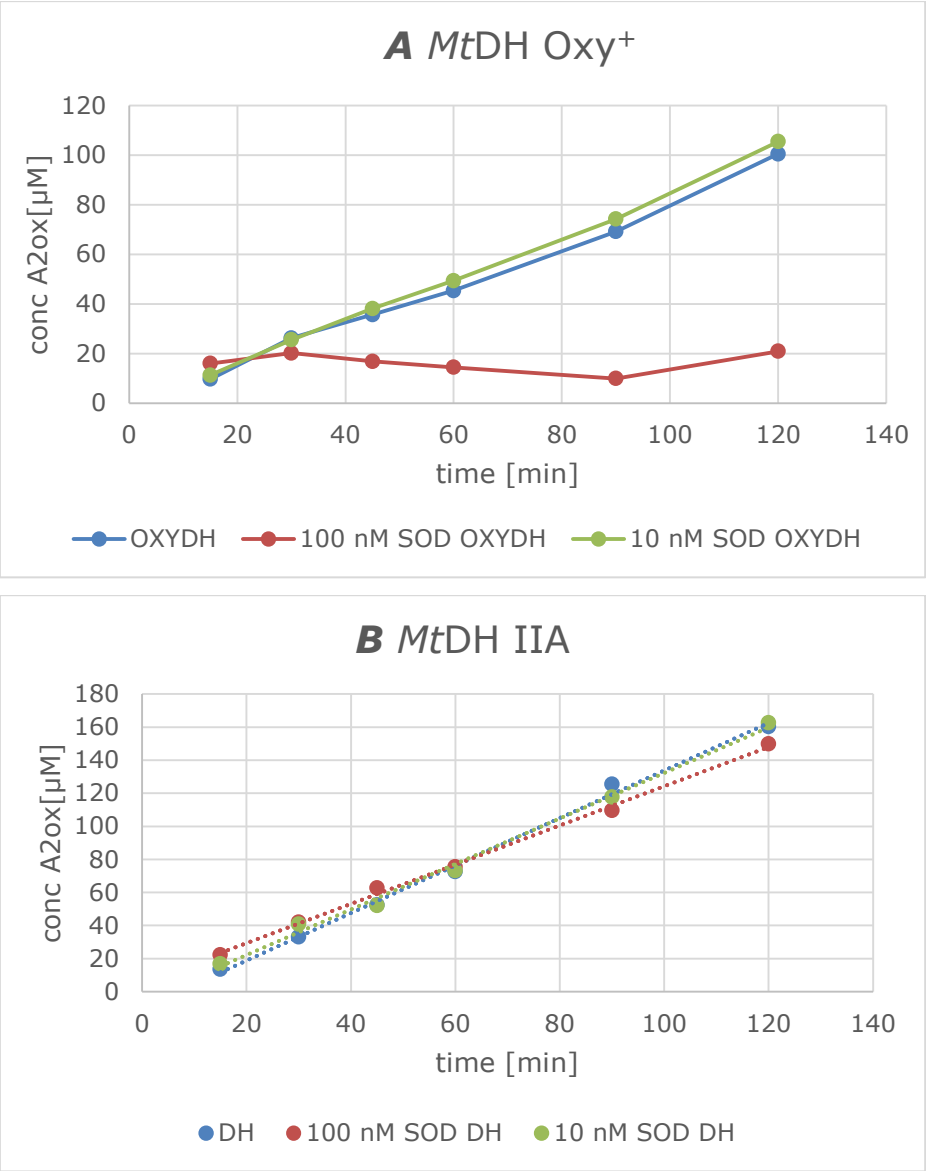

Figure 50. Influence of 10 and 100 nM SOD additions on product formation (no reductant present). (A) *Mt*DH Oxy^+ and (B) *Mt*DH IIA.

From these experiments it is obvious that superoxide does not affect the product formation of LPMO. H_2O_2seems to be not rate limiting.

If superoxide was formed at the experiment with *Mt*DH Oxy^+ in combination with 100 nM SOD, it could have been converted to high amounts of H_2O_2 causing inactivation of LPMO resulting in no observable products formation.

Leaking FAD hypothesis

Another investigated hypothesis was the leaking of reduced FAD from the DH domain, which could enable reduction of the LPMO. To date, the dissociation constant (K_d) of FAD binding to the DH domain of CDH is not known.

A potentially enabling activation of the LPMO by another H_2O_2- producing enzyme, the P2O (pyranose 2-oxidase), that is known to covalently bind the FAD cofactor (no leakage of FAD), was tested to activate the LPMO in presence and absence of ascorbic acid.

P2O reaction:

D-glucose + O_2 → 2-dehydro-D-glucose + H_2O_2

Three sets of experiments were performed. In the first one, P2O (concentrations ranging from 1.5µM to 7.8 nM), glucose as substrate, β-chitin and CBP21 were employed. In the second one, P2O and glucose were incubated with β-chitin, CBP21 and ascorbic acid. In the last series, CBP21, β-chitin and FAD in a range of concentrations replaced the reductant. The HPLC results showed two unknown peaks potentially corresponding to 2-dehydro-D-glucose.

As FAD was increased to 1.75 mM, 1 mM or 0.5 mM FAD low amounts of products got visible after 24 h incubation in the dark. This is shown in Table 11.

Table 11. FAD causing activation of LPMO in the dark.

	conc A2Ox [µM]
24h 1,75 mM FAD	7,4
24h 1 mM FAD	4,5
24h 0,5 mM FAD	3,2
In comparison:	
24 h WT and CBP21	1071,0

The highest concentration of wil-type DH used was 1.5 µM in reactions lacking ascorbic acid. Under these conditions,it was still able to reduce LPMO.

As free FAD needs to be reduced to act as electron donor for LPMO another experiment, to test the effect of FAD on the activation of LPMOs was performed. CBP21 was incubated with β-chitin in the presence or absence of FAD and

*Pc*P2O/glucose or *Mt*DH IIA/lactose in 50 mM phosphate buffer, pH 6. As a positive control 1 mM ascorbic acid was added to CBP21.

Table 12. Testing leaking FAD hypothesis; experimental setup.

***Pc*P2O**	***Mt*DH IIA**	**CBP21**	**FAD**	**Lactose/Glucose**	**Chitin**
x	1,5 µM	1 µM	0.5 mM	15 mM	10 g/L
x	1,5 µM	1 µM	x	15 mM	10 g/L
100 nM	x	1 µM	0.5 mM	15 mM	10 g/L
100 nM	x	1 µM	x	15 mM	10 g/L

*Pc*P2O or *Mt*DH IIA could, in addition to the production of H_2O_2, reduce FAD which in turn could activate the LPMO. As *Pc*P2O alone is only able to produce H_2O_2, but is unable to directly activate the LPMO, the expected outcome is a lack of products in this experimental setup. On the other hand, if reduced FAD is present, product formation would be expected. For *Mt*DH IIA, which can activate LPMOs without an external electron donor present (e.g. ascorbic acid or the additional cytochrome-b domain), the presence of free FAD in the reaction is hypothesized to cause a beneficial effect in activation of the LPMO

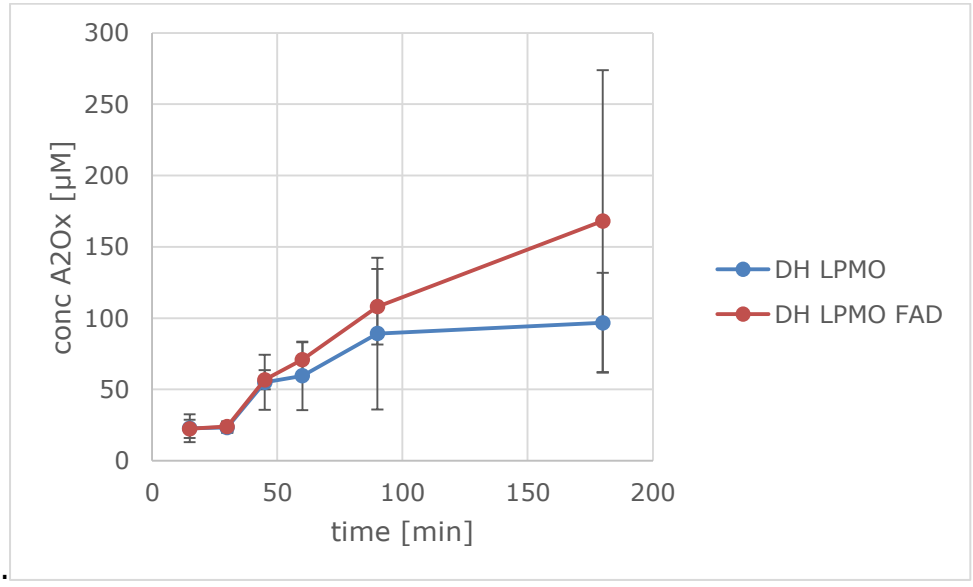

Figure 51. Chitobionic acid formation; influence of FAD.

All reactions were performed in triplicates. No products were observed in reactions containing *Pc*P2O/glucose during the first six-time points. After 24 h, small amounts of LPMO products were observed for both reactions, i.e. with and without addition of FAD, indicating that the presence of FAD does not stimulate the activity of LPMO in those reactions. For the *Mt*DH IIA/lactose system, it

seemed that addition of FAD is at least beneficial for LPMO activity (red curve with *Mt*DH IIA and FAD in figure 49 vs blue curve without FAD) but the high standard deviation does not allow to draw an ultimate conclusion.

Reducing sugar hypothesis

Another hypothesis why LPMO is activated by the DH-domain without adding any reductant could be the usage of high concentrations of reducing sugars (i.e. lactose) or low concentration of leaking FAD in combination with an enzyme that provides the LPMO with H_2O_2 (i.e. CDH)

As a negative control, only chitin 10 g/L, 1 µM CBP21 and 100 µM H_2O_2 were provided. This lead to low amounts of products according to literature (11), which can be seen in Figure 51 . As a positive control a standard reaction with 1 mM ascorbic acid was added to chitin and 1 µM CBP21 which lead to high product yields. Different possible reductants were tested. All samples contained chitin and CBP21 and were performed in 50 mM Bis-Tris buffer, pH 6.0. Lactose, glucose, FAD and ascorbic acid were tested with and without addition of H_2O_2. All reactions were incubated for 72 h.

If the reducing agents would cause the activation of the enzyme, the products formed by the LPMO in the negativ controls should be lower than in the sample which contain possible reducing agents and H_2O_2. The samples containing only reducing agent but no H_2O_2 should result in no product formation.

As shown in the graphs below in Figure 52, it seems likely that lactose in combination with H_2O_2 slightly boosted the production of chtiobionic acid, as well as did the addition of ascorbic acid. On the other hand product formation was very low, which means that the reducing sugar lactose cannot be the only reductant causing the high product formation of LPMO seen when using only DH.

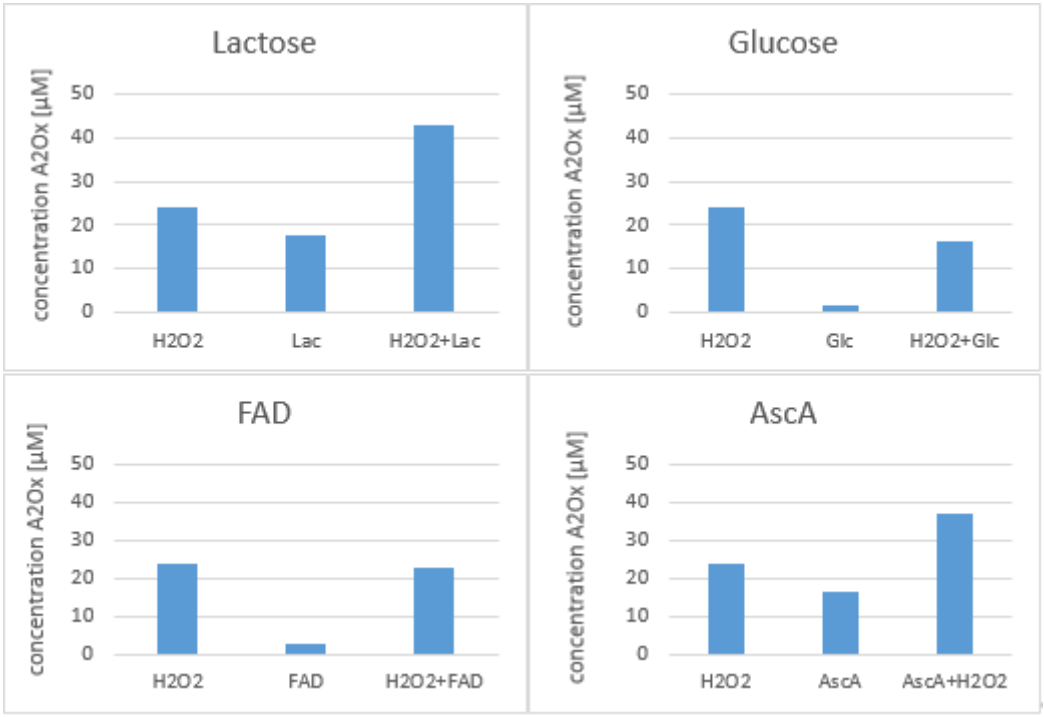

Figure 52. Testing the reducing sugar hypothesis.

2.3.2.9 Time course: activation of CBP21 with all CDH variants and the effect of ascorbic acid

The following experiments aimed to investigate the time courses of all CDH variants in reactions containing CBP21 with and without the reducing agent ascorbic acid. All reactions were performed in triplicate and employed either 1500 nM *Mt*CDH IIA and *Mt*DH IIA, or 31.24 nM *Mt*CDH Oxy^+ and *Mt*DH Oxy^+. All reactions contained 1 µM LPMO, 10 g/L chitin and 15 mM lactose. One series of experiments was performed with and one without ascorbic acid. Samples were incubated at 40 degrees and shaking at 1000 rpm. (Figure 53)

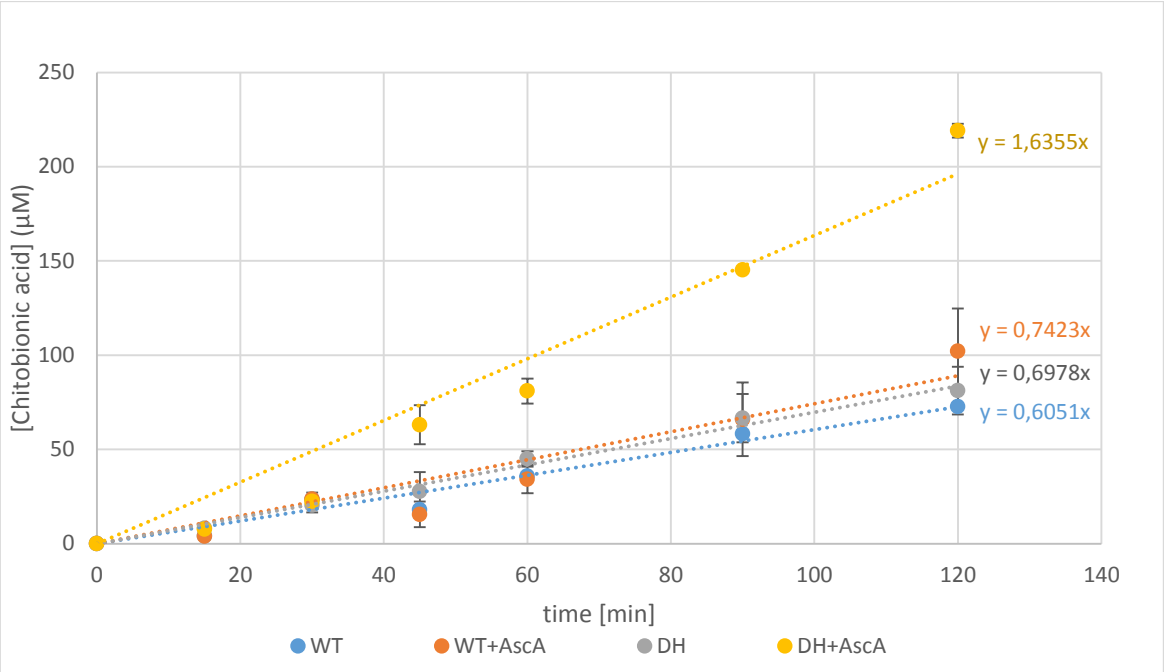

Figure 53. Time course: wild-type CDH and wild-type DH with and without ascorbic acid.

The presence of ascorbic acid in reactions containing the full-length CDH in combination with CBP21 did not influence product formation significantly. Added of ascorbic acid to the DH domain lead to a two-fold higher product release by CBP21. (Figure 54)

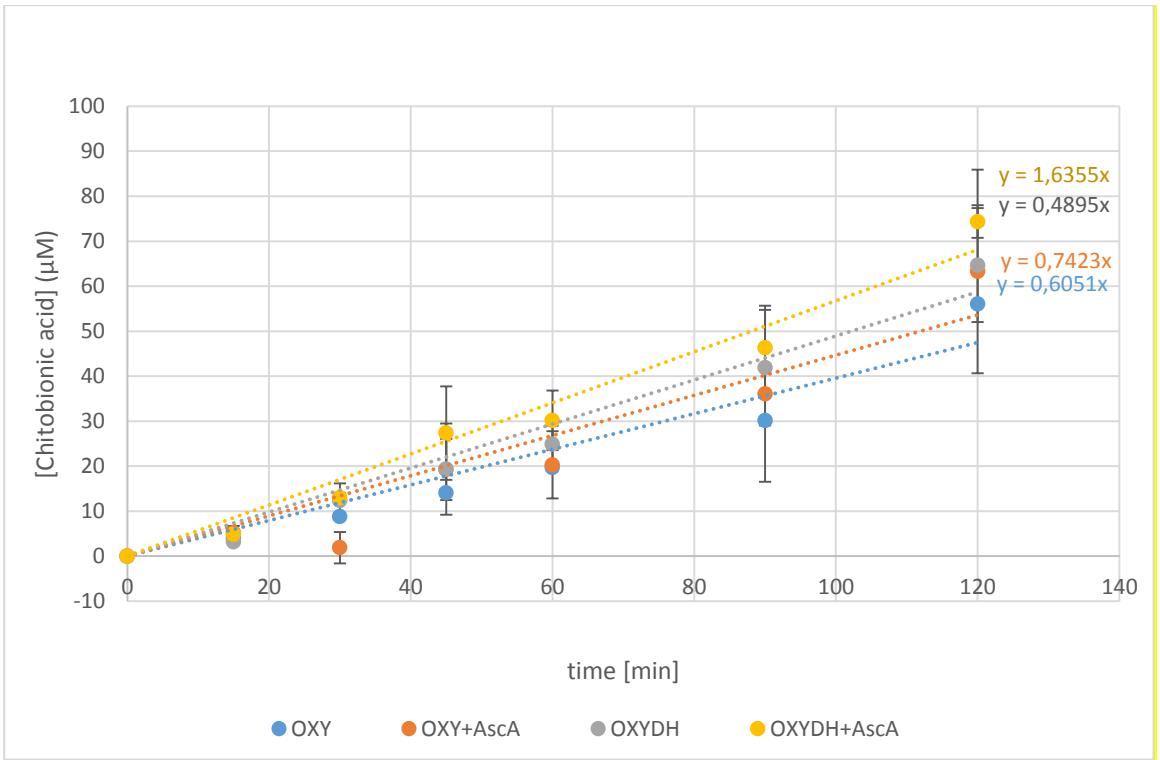

Figure 54. Time course; OXY-CDH and OXY-DH with and without ascorbic acid.

A different picture emerged when the variants *Mt*CDH Oxy$^+$ and *Mt*DH Oxy$^+$. were used. Here, addition of ascorbic acid had no apparent influence on the product formation.

Chitin caused reduction of LPMO

To exclude chitin as a possible electron supplier for LPMO, a cellulose-active LPMO was tested in combination with *Mt*DH Oxy$^+$ and *Mt*DH IIA with and without ascorbic acid on PASC. Ractions contained 1 µM LPMO; 1.5µM *Mt*DH IIA and 31.25 nM *Mt*DH Oxy$^+$ in 50 mM phosphate buffer, pH XY. PASC was used at a concentration of 0.2 %. ascorbic acid and lactose were added to 100 µM and 15mM, respectively. (Figure 55)

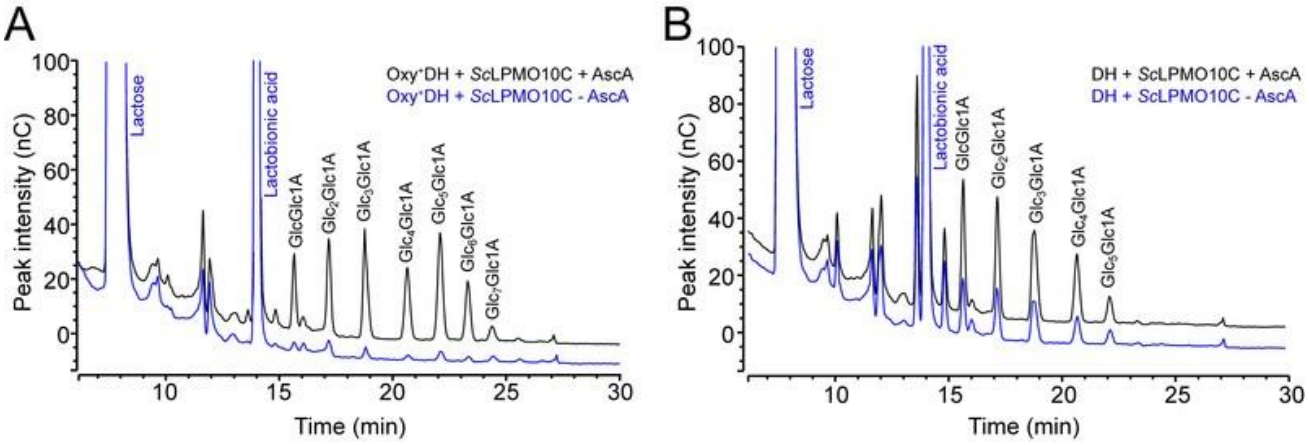

Figure 55. HPAEC spectra; product profiles ScLPMO10C and *Mt*DH Oxy$^+$ or *Mt*DH IIA.

Since products were detected for the cellulose-active LPMO, even in absence of ascorbic acid, chitin cannot cause activation of LPMO. It seems like ascorbic acid has a beneficial effect in activation of LPMO as higher peaks are seen in black (Figure 55). In picture B Glc_6Glc1A and Glc_7Glc1A are missing due to an endoglucanase activity. Samples were taken after 4 h.

2.3.2.10 Dose response experiment: NcLPMO9c on PASC

The same dose response experiment was also performed with *Nc*LPMO9C.

To test the interaction between *Nc*LPMO9c and CDH, and to validate the electrochemical experiments, different ratios of CDH to *Nc*LPMO9C were

incubated and products analyzed. The concentration of *Nc*LPMO9c was kept at 1 µM while the concentration of CDH was varied from 3, 1.5, 1, 0.5, 0.25, 0.125, 0.03125, 0.015625 and 0.0078125 µM.

Both full length CDHs, *Mt*CDH IIA and *Mt*CDH Oxy^+, were used. Ten g/L β-chitin was used as substrate for CBP21, and 15 mM lactose as substrate for the CDHs was added. Incubation was performed 24 h at 40 °C and 1000 rpm. 60 µL samples were taken after 1 h and 24 h. The samples were inactivated by the addition of sodium hydroxide (35 µL sample + 35 µL NaOH 1M). After centrifugation samples were ready to be analyzed at HPAEC.

With increasing amount of *Mt*CDH Oxy^+, C4 oxidized products of the LPMO are further oxidized to double oxidized products. This effect makes it impossible to integrate peak areas. As shown in Figure 56, 7.8 nM *Mt*CDH Oxy^+ were still able to activate LPMO9Cc.

Figure 56. HPLC profile; different ratios of LPMO9C to OXY+; with increasing OXY content double oxidized products dominate.

3 Conclusion and Outlook

In the present work an electrochemical screening method was developed to follow the time-dependent H_2O_2 consumption of *Nc*LPMO9C. Two different electron suppliers, ascorbic acid and CDH could both activate the enzyme efficiently. All experiments were performed under nitrogen atmosphere, which means that the availability of oxygen as a co-substrate was limited. Oxygen was thought to be the substrate of LPMOs for years. However, using this electrochemical method in combination with HPAEC analysis of the reaction products, we could verify the results of a recently published paper by Bissaro et al. (21) suggest that H_2O_2 is an alternative co-substrate for LPMO. We could confirm these hypothesis findings by showing that only reductant, cellulose and H_2O_2 are needed to activate *Nc*LPMO9C. Notably, only 1 µmol of reductant (ascorbic acid) was needed to deplete 7.4-12.5 µmol of peroxide. This also illustrates that the peroxide feeding rate is an important aspect in this reaction. It was shown that excess of H_2O_2 can be detrimental for the enzyme, leading to severe autooxidation (REF Bastien). Here, high amounts of peroxide (50 and 100 µM) were added batch-wise to the reations. Future experiments employing controlled feeding rates will be needed to test the stability of the reaction and to establish regimes with stable reaction kinetics. As the experiments were reproducible and repeatable, this method is very promising to gain more interesting kinetic data of different LPMOs.

Since the activation of LPMOs using CDH as H_2O_2 provider was of special interest, we tested different ratios of CDH concentrations relative to LPMO concentration and found that the optimal ratio of CDH to LPMO was one to one as the catalytic rate was reduced with lower amounts of CDH. The consumption of H_2O_2 either by using CDH or adding ascorbic acid as reductant took only a couple of sec.

In the second part of this work, four different variants of CDH (*Mt*CDH IIA, *Mt*DH IIA, *Mt*CDH Oxy^+, *Mt*DH Oxy^+) in combination with the chitin-active CBP21 and the cellulose-active *Nc*LPMO9C were tested by quantitatively measuring their products using different HPLC methods. *Mt*CDH Oxy^+ is a CDH with higher affinity to oxygen producing higher amounts in H_2O_2.

As CDH oxidizes the products of *Nc*LPMO9C, we tried to prevent this effect with addition of high amounts of another substrate for CDH i.e. lactose. Unfortunately, it was still not possible to control the oxidation of LPMO products by the OXY^+ variants. Due to the problematic product analysis of the cellulose active LPMO in combination with CDH, we used CBP21 (syn.*Sm*LPMO10A).

The results show that the concentration of *Mt*CDH Oxy^+ could be reduced about 47 times relative to the optimal *Mt*CDH IIA concentration while still generating similar amounts of LPMO reaction products. The amounts of formed products were shown to be proportional to the H_2O_2production rate by the CDH variants, in which the *Mt*CDH Oxy^+ was 240 times more efficient than the wild-type enzyme. This discovery makes the use of LPMOs in combination with CDH more interesting for industrial applications as CDH can activate the active site-copper and fuel the LPMO with H_2O_2 in a controlled, non-destructing way.

As enzymes are very expensive, reducing the amounts of enzymes in an industrial process by a factor of 47 would lead to enormous cost savings. As different types of LPMOs are reactive on different substrates like cellulose, chitin and starch, it makes them very attractive biocatalysts for the degradation of a broad range of resources to produce biofuel or other bio-based.

*Mt*CDH IIA that was used in this study is consists of three domains (CYT-DH-CBM1) as described earlier. Previous studies have shown that both the CYT and the DH of CDH are needed to activate LPMOs. The DH domain is necessary to generate H_2O_2 while CYT has been shown to deliver electrons to activate LPMOs. Two variants *Mt*DH IIA and *Mt*DH Oxy^+ containing only the DH domain and the CBM1 were also able to activate LPMOs. CYT in CDH donates electrons very fast to the LPMO active site, which was not seen for the DH domain so far. It can be speculated that activation of LPMO by DH underlies a different mechanism that happens much slower. These variants produced twice as much H_2O_2 when compared to the two full lengths CDHs. This could be caused by the presence of the CYT domain which could partly block the active site in DH and make it more difficult for oxygen to enter. The CYT domain withdraws electrons from the DH domain during catalysis, which means less electrons are available and therefore less H_2O_2 is produced.

To rationalize this effect, three different hypotheses were tested: 1.) Formation of superoxide by CDH as inducer of LPMO; 2.) The leaking of reduced FAD cofactor from CDH or 3.) the high amounts of lactose, whose reducing ends could potentially act as a weak reductant for LPMO. Both, the FAD hypothesis as well as the superoxide formation hypothesis had indications causing the activation of LPMO, but the data were not significant enough to strengthen these hypotheses. More research in finding a hypothesis why activation is possible needs to be done in future work.

The newly developed electrochemical method to analyse H_2O_2 consuming reactions offers great potential to gain a lot more kinetic data of enzymes. In future experiments CDH is a very promising enzyme in activating LMPO, because it is not only activating moreover it supplies LMPO with H_2O_2. A very interesting question which came up in this work, as we found out that that LPMO can be activated by only short lengths CDHs, is why fungi invests so much energy to produce full-lengths CDHs without gaining any positive effect The full lengths CDH seems to have other benefits for the fungus we don’t know so far. It could drive faster reactions or could cause a more specific activation.
The main interest in future projects should be how these findings could be incorporated into the biofuel industry to provide alternative energy sources and push back fossil fuels.

List of figures

Tables

References

1. Henrich E, Dahmen N, Dinjus E, Sauer J. The Role of Biomass in a Future World without Fossil Fuels. Chem Ing Tech. 2015 Dec;87(12):1667–85.

2. Hemsworth GR, Johnston EM, Davies GJ, Walton PH. Lytic Polysaccharide Monooxygenases in Biomass Conversion. Trends Biotechnol. 2015 Dec;33(12):747–61.

3. Agger JW, Isaksen T, Varnai A, Vidal-Melgosa S, Willats WGT, Ludwig R, et al. Discovery of LPMO activity on hemicelluloses shows the importance of oxidative processes in plant cell wall degradation. Proc Natl Acad Sci. 2014 Apr 29;111(17):6287–92.

4. Kracher D, Ludwig R. Cellobiose dehydrogenase: An essential enzyme for lignocellulose degradation in nature – A review / Cellobiosedehydrogenase: Ein essentielles Enzym für den Lignozelluloseabbau in der Natur – Eine Übersicht. Bodenkult J Land Manag Food Environ [Internet]. 2016 Jan 1 [cited 2017 Aug 19];67(3). Available from: https://www.degruyter.com/view/j/boku.2016.67.issue-3/boku-2016-0013/boku-2016-0013.xml

5. Cellulose [Internet]. [cited 2017 Nov 15]. Available from: http://www1.lsbu.ac.uk/water/cellulose.html

6. Scheller HV, Ulvskov P. Hemicelluloses. Annu Rev Plant Biol. 2010 Jun 2;61(1):263–89.

7. Horn S, Vaaje-Kolstad G, Westereng B, Eijsink VG. Novel enzymes for the degradation of cellulose. Biotechnol Biofuels. 2012;5(1):45.

8. Nanda S, Mohammad J, Reddy SN, Kozinski JA, Dalai AK. Pathways of lignocellulosic biomass conversion to renewable fuels. Biomass Convers Biorefinery. 2014 Jun;4(2):157–91.

9. Vaaje-Kolstad G, Forsberg Z, Loose JS, Bissaro B, Eijsink VG. Structural diversity of lytic polysaccharide monooxygenases. Curr Opin Struct Biol. 2017 Jun;44:67–76.

10. Danneels B, Tanghe M, Joosten H-J, Gundinger T, Spadiut O, Stals I, et al. A quantitative indicator diagram for lytic polysaccharide monooxygenases reveals the role of aromatic surface residues in HjLPMO9A regioselectivity. Berrin J-G, editor. PLOS ONE. 2017 May 31;12(5):e0178446.

11. Vaaje-Kolstad G, Westereng B, Horn SJ, Liu Z, Zhai H, Sorlie M, et al. An Oxidative Enzyme Boosting the Enzymatic Conversion of Recalcitrant Polysaccharides. Science. 2010 Oct 8;330(6001):219–22.

12. Johansen KS. Discovery and industrial applications of lytic polysaccharide mono-oxygenases. Biochem Soc Trans. 2016 Feb 15;44(1):143–9.

13. Isaksen T, Westereng B, Aachmann FL, Agger JW, Kracher D, Kittl R, et al. A C4-oxidizing Lytic Polysaccharide Monooxygenase Cleaving Both Cellulose and Cello-oligosaccharides. J Biol Chem. 2014 Jan 31;289(5):2632–42.

14. Levasseur A, Drula E, Lombard V, Coutinho PM, Henrissat B. Expansion of the enzymatic repertoire of the CAZy database to integrate auxiliary redox enzymes. Biotechnol Biofuels. 2013;6(1):41.

15. Lombard V, Golaconda Ramulu H, Drula E, Coutinho PM, Henrissat B. The carbohydrate-active enzymes database (CAZy) in 2013. Nucleic Acids Res. 2014 Jan;42(D1):D490–5.

16. Morgenstern I, Powlowski J, Tsang A. Fungal cellulose degradation by oxidative enzymes: from dysfunctional GH61 family to powerful lytic polysaccharide monooxygenase family. Brief Funct Genomics. 2014 Nov 1;13(6):471–81.

17. Loose JSM, Forsberg Z, Kracher D, Scheiblbrandner S, Ludwig R, Eijsink VGH, et al. Activation of bacterial lytic polysaccharide monooxygenases with cellobiose dehydrogenase: Activation of Bacterial LPMOs with CDH. Protein Sci. 2016 Dec;25(12):2175–86.

18. Vaaje-Kolstad G, Horn SJ, van Aalten DMF, Synstad B, Eijsink VGH. The Non-catalytic Chitin-binding Protein CBP21 from *Serratia marcescens* Is Essential for Chitin Degradation. J Biol Chem. 2005 Aug 5;280(31):28492–7.

19. Phillips CM, Beeson WT, Cate JH, Marletta MA. Cellobiose Dehydrogenase and a Copper-Dependent Polysaccharide Monooxygenase Potentiate Cellulose Degradation by *Neurospora crassa*. ACS Chem Biol. 2011 Dec 16;6(12):1399–406.

20. Kracher D, Scheiblbrandner S, Felice AK, Breslmayr E, Preims M, Ludwicka K, et al. Extracellular electron transfer systems fuel cellulose oxidative degradation. Science. 2016;352(6289):1098–1101.

21. Bissaro B, Røhr ÅK, Müller G, Chylenski P, Skaugen M, Forsberg Z, et al. Oxidative cleavage of polysaccharides by monocopper enzymes depends on H2O2. Nat Chem Biol [Internet]. 2017 Aug 28 [cited 2017 Sep 5]; Available from: http://www.nature.com/doifinder/10.1038/nchembio.2470

22. Loose JSM, Forsberg Z, Fraaije MW, Eijsink VGH, Vaaje-Kolstad G. A rapid quantitative activity assay shows that the *Vibrio cholerae* colonization factor GbpA is an active lytic polysaccharide monooxygenase. FEBS Lett. 2014 Sep 17;588(18):3435–40.

23. Cox MC, Rogers MS, Cheesman M, Jones GD, Thomson AJ, Wilson MT, et al. Spectroscopic identification of the haem ligands of cellobiose oxidase. FEBS Lett. 1992 Jul 28;307(2):233–6.

24. Martin Hallberg B, Henriksson G, Pettersson G, Divne C. Crystal structure of the flavoprotein domain of the extracellular flavocytochrome cellobiose dehydrogenase. J Mol Biol. 2002 Jan;315(3):421–34.

25. Samejima M, Phillips RS, Eriksson K-EL. Cellobiose oxidase from *Phanerochaete chrysosporium* Stopped-flow spectrophotometric analysis of pH-dependent reduction. FEBS Lett. 1992 Jul 20;306(2–3):165–8.

26. Rytioja J, Hildén K, Yuzon J, Hatakka A, de Vries RP, Mäkelä MR. Plant-Polysaccharide-Degrading Enzymes from Basidiomycetes. Microbiol Mol Biol Rev. 2014 Dec;78(4):614–49.

27. Langston JA, Shaghasi T, Abbate E, Xu F, Vlasenko E, Sweeney MD. Oxidoreductive Cellulose Depolymerization by the Enzymes Cellobiose Dehydrogenase and Glycoside Hydrolase 61. Appl Environ Microbiol. 2011 Oct 1;77(19):7007–15.

28. Nicholson RS. Theory and Application of Cyclic Voltammetry for Measurement of Electrode Reaction Kinetics. Anal Chem. 1965;37(11):1351–1355.

29. | PD 02 S 2011 |Updated: 02-S-2011 |Category: E |Author: THW |Member LG |Points: 12. Electrochemical cell, its working principle, setup and representation. [Internet]. India Study Channel. 2011 [cited 2017 Oct 18]. Available from: http://www.indiastudychannel.com/resources/144686-Electrochemical-cell-its-working-principle-setup-and-representation.aspx

30. H_2O_2 electrochemistry on platinum: Towards understanding the oxygen reduction reaction mechanism [Internet]. ResearchGate. [cited 2017 Oct 18]. Available from: https://www.researchgate.net/publication/224770048_Hydrogen_peroxide_electrochemistry_on_platinum_Towards_understanding_the_oxygen_reduction_reaction_mechanism

31. Autolab_Application_Note_EC08.pdf.

32. Principles of MALDI-TOF Mass Spectrometry : SHIMADZU (Shimadzu Corporation) [Internet]. [cited 2017 Sep 15]. Available from: http://www.shimadzu.com/an/lifescience/maldi/princpl1.html

33. Bissaro B, Rohr AK, Skaugen M, Forsberg Z, Horn SJ, Vaaje-Kolstad G, et al. Fenton-type chemistry by copper enzyme: molecular meachanism of polysaccharide oxidative cleavage.

34. Kittl R, Kracher D, Burgstaller D, Haltrich D, Ludwig R. Production of four Neurospora crassa lytic polysaccharide monooxygenases in Pichia pastoris monitored by a fluorimetric assay. Biotechnol Biofuels. 2012;5(1):79.

Index of abbreviations

CBP21	Lytic polysaccharide monooxygenase *10A* from *Serratia marcescens*
CDH	cellobiose dehydrogenase
Cels2	Lytic polysaccharide monooxygenase *10C Streptomyces coelicolor*
DP	degree of polymerization
h	hours
H_2O_2	hydrogen peroxid
Glc	glucose
Glc2	cellobiose
Glc3	cellotriose
Glc6	cellohexaose
GlcNac	N-acteylglucosamin
LPMO	lytic polysaccharide monooxygenase
MALDI-TOF	*matrix-assisted-laser-desorption/Ionisation- time of flight*
min	minute
*Mt*CDH IIA	cellobiose dehydrogenase (*Myriococcum thermophilum*)
*Mt*DH IIA	cellobiose dehydrogenase which only has a dehydrogenase domain and no cytochrome domain *(Myriococcum thermophilum*)
*Mt*CDH Oxy^+	cellobiose dehydrogenase for improved hydrogen peroxideproduction (*Myriococcum thermophilum*)

*Mt*DH Oxy^{+}	cellobiose dehydrogenase for improved hydrogen peroxideproduction, which only has a dehydrogenase domain and no cytochrome domain (*Myriococcum thermophilum*)
*Nc*LPMO9c	Lytic polysaccharide monooxygenase *9C* from *Neurospora crassa*
PASC	phosphoric acid swollen cellulose
*Pc*P2O	*Phanerochaete chrysosporium* pyranose 2 oxidase
Rpm	rounds per minute
S	second
SOD	superoxide dismutase
Std. Dev.	Standard deviation